MECHANISTIC DESIGN DATA FROM ODOT INSTRUMENTED PAVEMENT SITES

Phase 1 Report

SPR 763

MECHANISTIC DESIGN DATA FROM ODOT INSTRUMENTED PAVEMENT SITES

Phase 1 Final Report

SPR 763

by
David H. Timm, P.E.
Michael C. Vrtis
National Center for Asphalt Technology (NCAT)
Auburn University
277 Technology Parkway
Auburn, AL 36830

for

Oregon Department of Transportation
Research Section
555 13th Street NE, Suite 1
Salem OR 97301

and

Federal Highway Administration
1200 New Jersey Avenue SE
Washington, DC 20590

March 2017

Technical Report Documentation Page

1. Report No. FHWA	2. Government Accession No.	3. Recipient's Catalog No.
4. Title and Subtitle Mechanistic Design Data from ODOT Instrumented Pavement Sites		5. Report Date -March 2017- 6. Performing Organization Code
7. Author(s) David H. Timm, P.E., and Michael C. Vrtis		8. Performing Organization Report No. SPR 763 – Phase 1
9. Performing Organization Name and Address National Center for Asphalt Technology (NCAT) Auburn University 277 Technology Parkway Auburn, AL 36830		10. Work Unit No. (TRAIS) 11. Contract or Grant No.
12. Sponsoring Agency Name and Address Oregon Dept. of Transportation Research Section and Federal Highway Admin. 555 13th Street NE, Suite 1 1200 New Jersey Avenue SE Salem, OR 97301 Washington, DC 20590		13. Type of Report and Period Covered Phase 1 Final Report 14. Sponsoring Agency Code

15. Supplementary Notes

16. Abstract

This investigation examined data obtained from three previously-instrumented pavement test sites in Oregon. Data processing algorithms and templates were developed for each test site that facilitated full processing of all the data to build databases representing each site. Investigation of site data found that most of the collected data could be successfully processed and observed trends in the data were as expected (e.g., seasonal changes affected pavement response). The location that compared rubblized base to aggregate base clearly demonstrated the effect of the rubblized base through a 50% reduction in strain at the bottom of the asphalt layer. Further investigations of the data may be warranted and user's guides provided in this report will enable those investigations to proceed by ODOT staff.

17. Key Words	18. Distribution Statement Copies available from NTIS, and online at http://www.oregon.gov/ODOT/TD/TP_RES/		
19. Security Classification (of this report) Unclassified	20. Security Classification (of this page) Unclassified	21. No. of Pages 56	22. Price

SI* (MODERN METRIC) CONVERSION FACTORS

APPROXIMATE CONVERSIONS TO SI UNITS

Symbol	When You Know	Multiply By	To Find	Symbol
		LENGTH		
in	inches	25.4	millimeters	mm
ft	feet	0.305	meters	m
yd	yards	0.914	meters	m
mi	miles	1.61	kilometers	km
		AREA		
in^2	square inches	645.2	millimeters squared	mm^2
ft^2	square feet	0.093	meters squared	m^2
yd^2	square yards	0.836	meters squared	m^2
ac	acres	0.405	hectares	ha
mi^2	square miles	2.59	kilometers squared	km^2
		VOLUME		
fl oz	fluid ounces	29.57	milliliters	ml
gal	gallons	3.785	liters	L
ft^3	cubic feet	0.028	meters cubed	m^3
yd^3	cubic yards	0.765	meters cubed	m^3
NOTE: Volumes greater than 1000 L shall be shown in m^3.				
		MASS		
oz	ounces	28.35	grams	g
lb	pounds	0.454	kilograms	kg
T	short tons (2000 lb)	0.907	megagrams	Mg
		TEMPERATURE (exact)		
°F	Fahrenheit	(F-32)/1.8	Celsius	°C

APPROXIMATE CONVERSIONS FROM SI UNITS

Symbol	When You Know	Multiply By	To Find	Symbol
		LENGTH		
mm	millimeters	0.039	inches	in
m	meters	3.28	feet	ft
m	meters	1.09	yards	yd
km	kilometers	0.621	miles	mi
		AREA		
mm^2	millimeters squared	0.0016	square inches	in^2
m^2	meters squared	10.764	square feet	ft^2
m^2	meters squared	1.196	square yards	yd^2
ha	hectares	2.47	acres	ac
km^2	kilometers squared	0.386	square miles	mi^2
		VOLUME		
ml	milliliters	0.034	fluid ounces	fl oz
L	liters	0.264	gallons	gal
m^3	meters cubed	35.315	cubic feet	ft^3
m^3	meters cubed	1.308	cubic yards	yd^3
		MASS		
g	grams	0.035	ounces	oz
kg	kilograms	2.205	pounds	lb
Mg	megagrams	1.102	short tons (2000 lb)	T
		TEMPERATURE (exact)		
°C	Celsius	1.8C+32	Fahrenheit	°F

*SI is the symbol for the International System of Measurement

ACKNOWLEDGEMENTS

The authors wish to thank the Oregon Department of Transportation for their support and cooperation with this project.

DISCLAIMER

This document is disseminated under the sponsorship of the Oregon Department of Transportation and the United States Department of Transportation in the interest of information exchange. The State of Oregon and the United States Government assume no liability of its contents or use thereof.

The contents of this report reflect the view of the authors who are solely responsible for the facts and accuracy of the material presented. The contents do not necessarily reflect the official views of the Oregon Department of Transportation or the United States Department of Transportation.

The State of Oregon and the United States Government do not endorse products of manufacturers. Trademarks or manufacturers' names appear herein only because they are considered essential to the object of this document.

This report does not constitute a standard, specification, or regulation.

TABLE OF CONTENTS

LIST OF FIGURES

LIST OF TABLES

1.0 INTRODUCTION

The Oregon DOT (ODOT) instrumented three pavement sites between 2004 and 2008 to support efforts toward implementing mechanistic-empirical (M-E) pavement design. These three sites are known as the Dever-Conner, Medford and Redmond test sites, respectively. The Dever-Conner and Medford sites are both located on I-5 while the Redmond site is on US 97 as depicted in Figure 1.1.

The purpose of the test sites was to support stepwise validation of the new M-E design approach under development by AASHTO. Specifically, ODOT was interested in measuring tensile strain at the bottom of asphalt concrete (AC) layers as a predictor for bottom-up fatigue cracking *(Scholz 2010).* These measurements were to provide validation of predictions made by computer programs using layered elastic theory.

Though data were collected as part of an earlier research project (Scholz, 2010), limited data reduction and analysis was conducted and much of the response measurement data are still considered to be in raw format. Therefore, there was a need to evaluate the usefulness of the data and assess whether it can be useful for M-E design. There was also a need to develop user-friendly tools for ODOT to continue collecting and analyzing data to support M-E design.

Given these needs, a research contract was awarded to the National Center for Asphalt Technology (NCAT) in 2014 with these main objectives:

1. Process existing data sets and evaluate their usefulness toward implementation of M-E design.

2. Develop user-friendly processing schemes to facilitate future data processing and analysis.

To achieve these objectives, the work was divided into two major phases. Phase I (Preliminary Evaluation) was meant to catalogue and assess the current state of the data, establish rudimentary processing schemes and execute some measured versus predicted strain response comparisons. The results of Phase I were intended to provide ODOT with sufficient information to make a decision whether to continue with Phase II (Full Evaluation). Phase II was to include full data processing and database development followed by technology transfer of the developed products.

The purpose of this report is to document the findings of Phase I as described in the following sections. Data procurement and processing scheme development are first detailed followed by the mechanistic analyses that were conducted. Conclusions and recommendations are then presented.

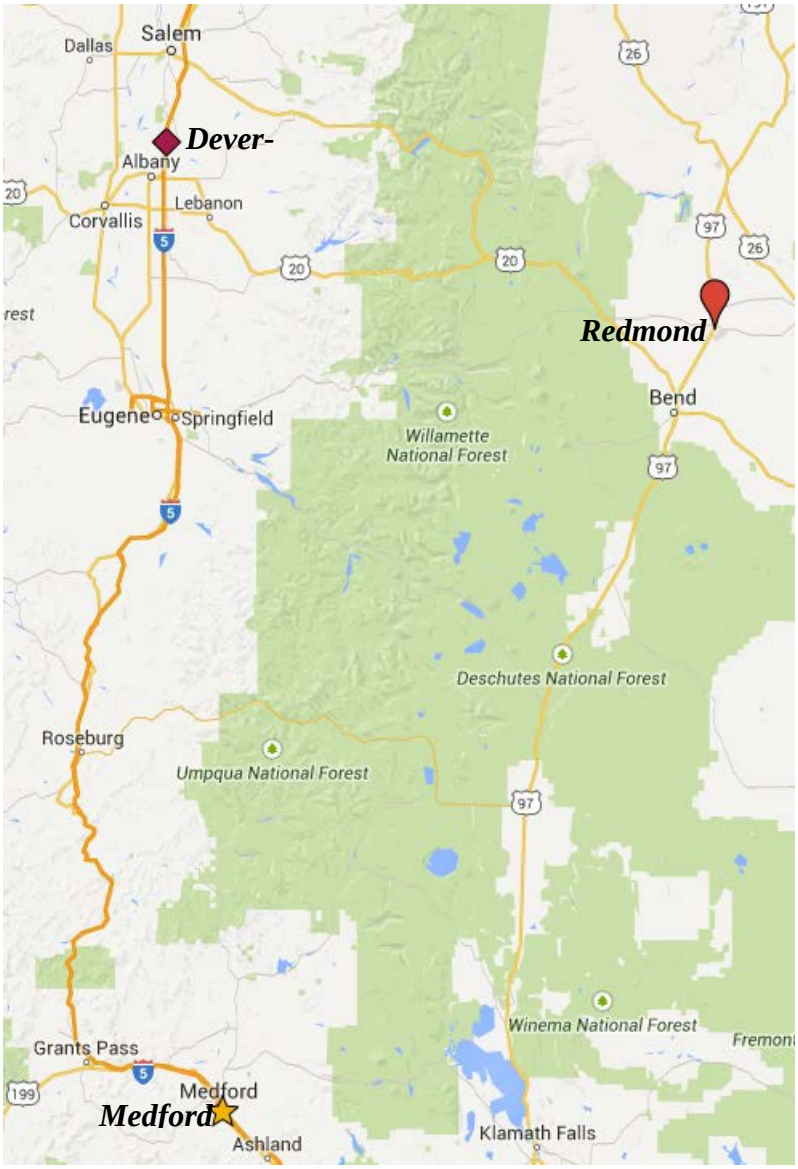

Figure 1.1: ODOT Instrumented Pavement Test Sites *(Google Earth 2015).*

2.0 DATA PROCUREMENT

ODOT provided DVD's containing project data to NCAT researchers at the start of the project. These included one DVD for the Medford site, six DVD's for the Dever-Conner site and two corresponding to the Redmond site. These discs were organized by test site and testing date as pictured in Figure 2.1. It is important to note that there was not a consistent set of information between the test sites or between test dates at a given test site. Any given test date or site contained any or all of the following:

- Raw strain files
- Processed strain files
- Weigh in motion (WIM) files
- Construction photos
- Photos of trucks during testing
- Field notes
- FWD Testing Data

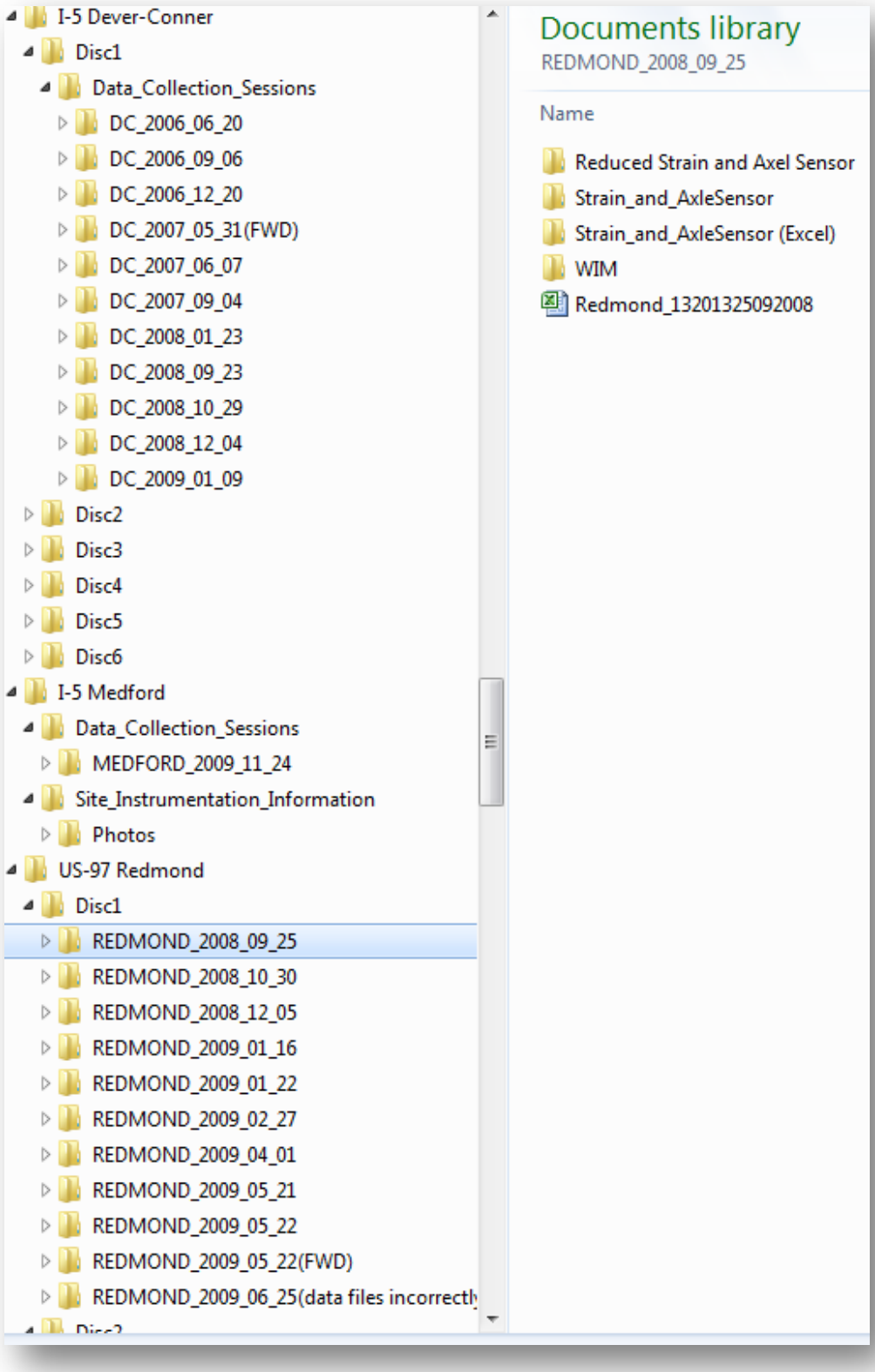

Figure 2.1: Data Organization.

After the data discs had been received, and a preliminary evaluation was conducted, a project kickoff meeting was held in Salem, OR. During this meeting, the data sets were discussed and the Dever-Conner site was visited. A main outcome of the meeting was general agreement to develop data processing schemes that featured minimal user interaction, utilized visual data inspection for quality control and output summary tables for future database development.

3.0 DATA PROCESSING SCHEME OVERVIEW

Before developing any processing schemes, the raw data files were investigated to determine the general format. It was found that every test site was a bit different, and even within a given test site, the file format tended to vary between testing dates. For example, some raw data were stored in text files, others in Excel files and others still in "TDMS" format which required a TDM importer from National Instruments to access the data within the file. Within the data files themselves, a variety of information was found with no widespread uniformity between files. The Redmond test site, for example, included some data files that had no timestamps associated with the measurements while other others included timestamps. The one common feature between the data files was that they appeared to correspond to a single truck pass in most cases. The data files for each test site will be fully described later in this report, but it is critical to understand that every deviation in data file requires a unique processing template.

While evaluating the data provided by ODOT, it was determined that the commercially-available program, DADiSP, was suitable for developing data processing schemes. Since it was found that the strain file format varied between test sites, and even between test dates at a given site, multiple processing templates had to be created in DADiSP. The processing templates were based on the gauge arrangements at each site as illustrated in Figure 3.1. Note that the Medford and Redmond sites had the same gauge arrangement consisting of three axle sensors to serve as a lateral positioning system (LPS) followed by an array of nine asphalt strain gauges (ASG). The ASG's were arranged to measure both longitudinal (with traffic) and transverse (perpendicular to traffic) strain. The Dever-Conner site had two arrays of twelve ASG's on either side of the LPS gauges. The first set (AB's) were placed on an aggregate base while the RB gauges were over a rubblized concrete base.

Despite differences between test sites or file configuration, the general processing approach was the same and followed the major steps listed below and described in the following subsections.

1. Clean all signals
2. Find all axle hits on surface mounted axle sensors
3. Calculate speed of each axle
4. Calculate axle spacing
5. Axle classification (steer, single, tandem, tridem, etc.)
6. Calculate offset from edge stripe using diagonal surface mounted axle sensor
7. Using speed of vehicle and gauge spacing, find peaks from each strain gauge
8. Tabulate data

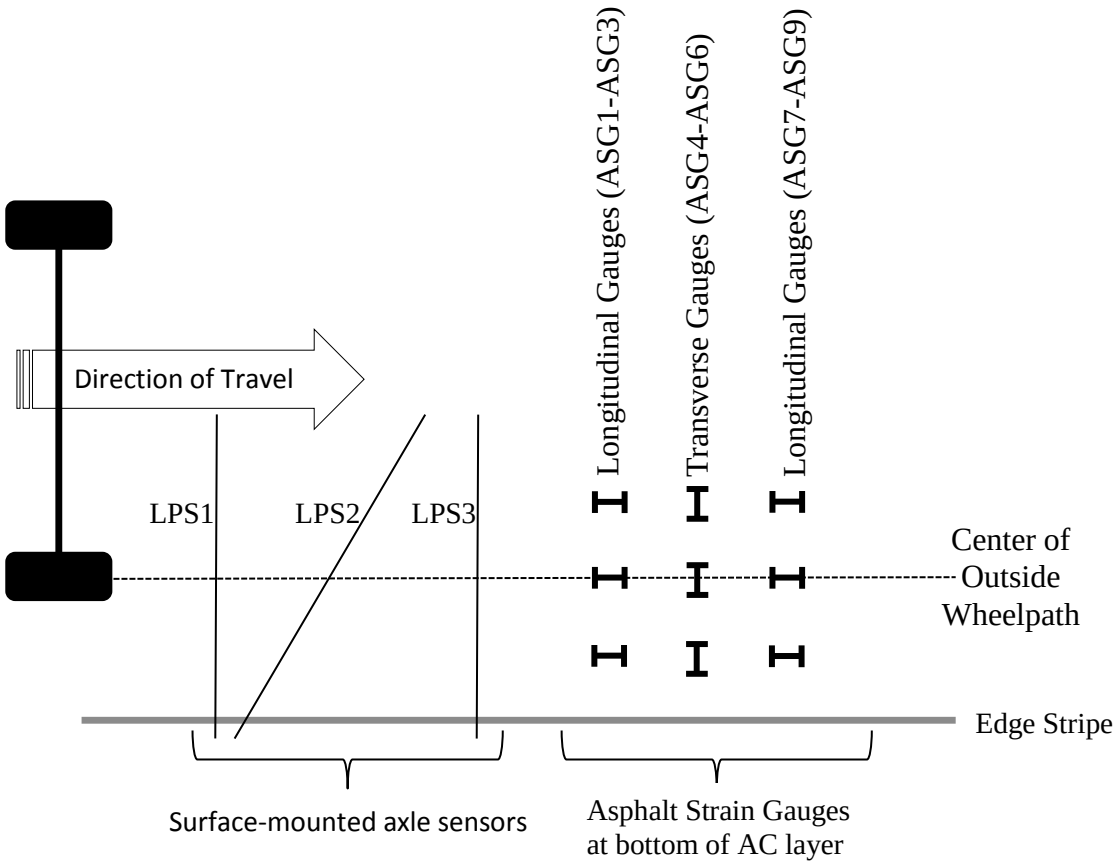

a) Redmond and Medford Test Sites

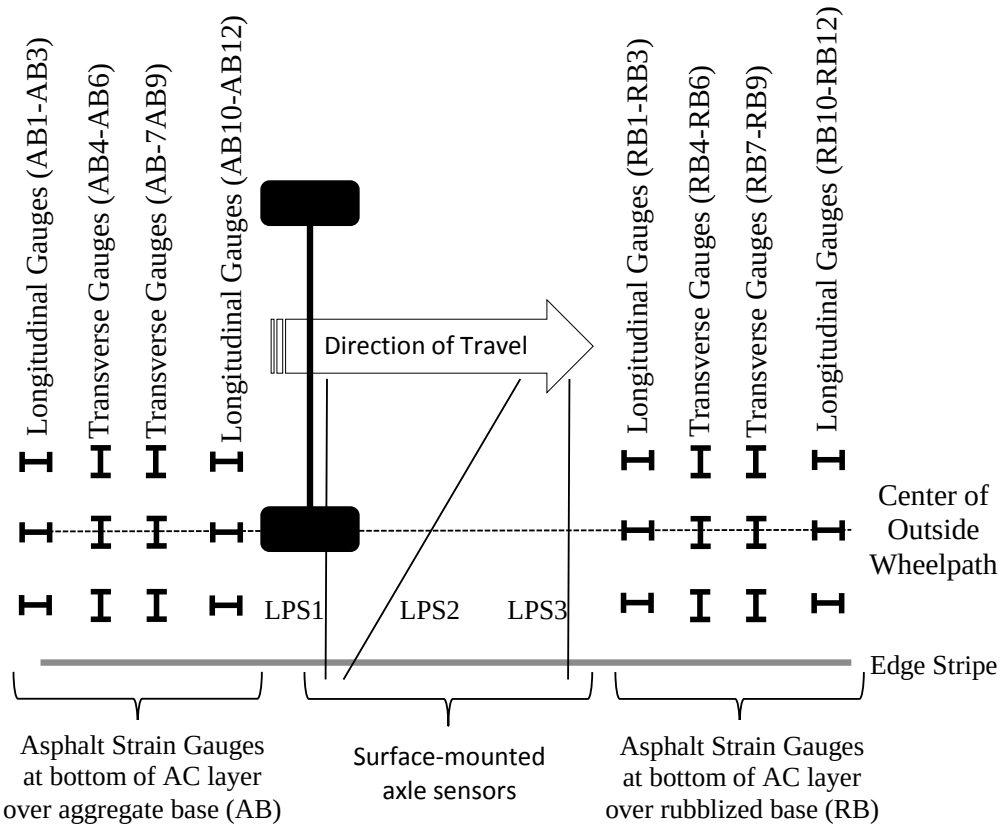

b) Dever-Conner Test Site

Figure 3.1: Test Site Gauge Arrangements (not to scale).

3.1 CLEAN ALL SIGNALS

An examination of the raw data indicated that no apparent real-time processing of the signals had been applied. An evaluation of the frequency spectrum of the raw data revealed that a single pole analog low pass filter with a 60 Hz cutoff frequency was effective in reducing noise without losing valuable information from the signal. Figure 3.2 illustrates a tandem axle event on an asphalt strain gauge that includes the raw and cleaned signal. The inset figure shows a magnified view of the signals.

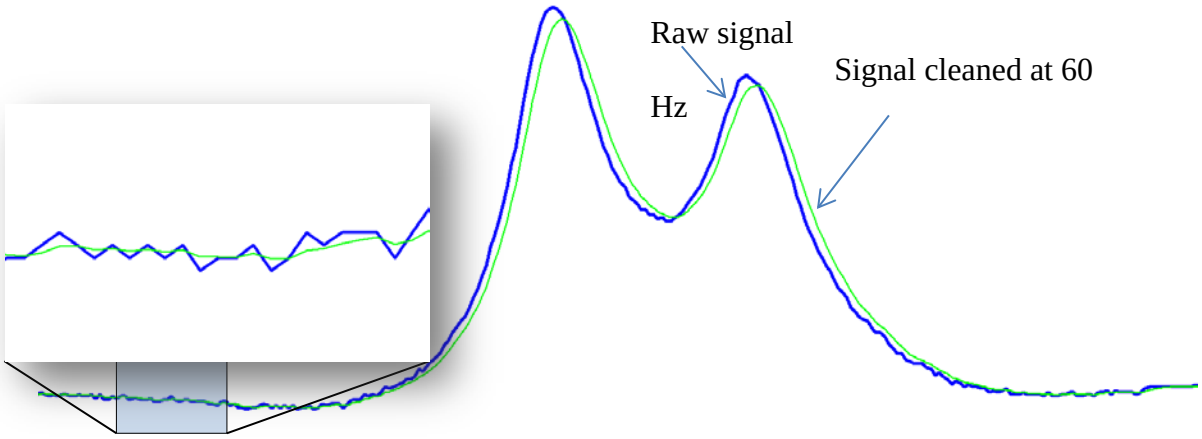

Figure 3.2: Raw and Cleaned Data Signal

3.2 FIND ALL LPS AXLE HITS

After cleaning all the raw data signals, the processing algorithms searched the LPS sensors to identify timestamps corresponding to individual axle hits. Figure 3.3 illustrates this procedure schematically where the truck is moving from right to left across the gauge array. The axle sensor diagram is inset in the figure and the voltage versus time signals are color coded to show each sensor separately. The steer axle corresponds to the first three voltage spikes on LPS1 (blue), LPS2 (green) and LPS3 (red). This axle event is followed by the next single axle on the truck. Interestingly, in this case, the diagonal sensor (LPS2) recorded a double hit before LPS3. This may be due to dual tires striking the diagonal gauge at distinct moments in time. For the purposes of data processing, the second spike should be ignored which is accomplished by using a minimum voltage threshold that constitutes a "good" axle hit. Finally, the rear tandem axle registers double hits on each sensor at which point the truck has moved past the instrumented area.

In terms of DADiSP processing, algorithms were written to search each signal and record each point in time when the previous voltage reading was below a predefined threshold (usually 1 volt) and the current point is above that threshold. These timestamps of each axle hit are critical to the remaining processing steps. Figure 3.4 illustrates sample output corresponding to the truck pass in Figure 3.3. The figure shows the axle number and corresponding voltage readings for each axle hit for this truck pass.

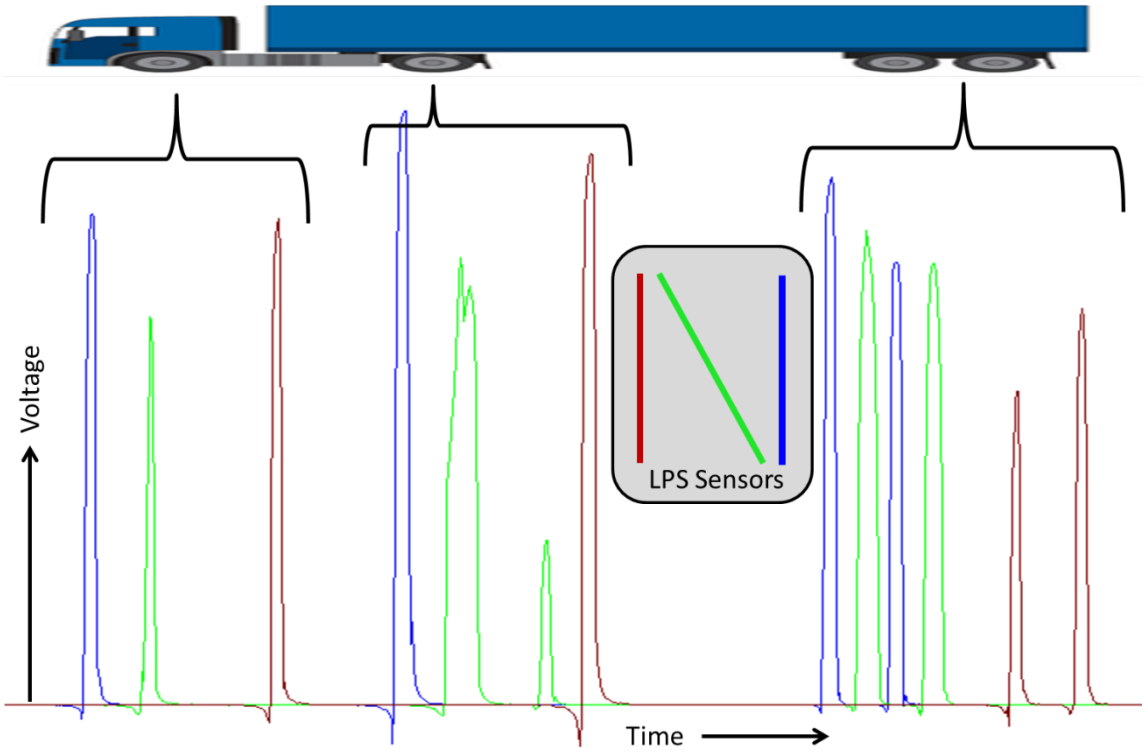

Figure 3.3: Sample Truck Pass Through LPS Gauge Array.

W27: LPS1-Axle Events

1: Axle	2: Voltage	3: Time,sec
1.000000	1.341473	0.276000
2.000000	1.197638	0.498000
3.000000	1.167479	0.805000
4.000000	1.392497	0.853000

W28: LPS2-Axle Events

1: Axle	2: Voltage	3: Time,sec
1.000000	1.362748	0.320000
2.000000	1.174051	0.536000
3.000000	1.090780	0.830000
4.000000	1.445561	0.879000

W29: LPS3-Axle Events

1: Axle	2: Voltage	3: Time,sec
1.000000	1.545753	0.410000
2.000000	1.665698	0.633000
3.000000	1.215787	0.941000
4.000000	1.314496	0.987000

Figure 3.4: Sample Truck Pass LPS Output from DADiSP.

3.3 DETERMINE SPEED OF EACH AXLE

Once the timestamps corresponding to each axle are determined from the previous step and tabulated as shown in Figure 3.4, the known physical distance between LPS1 and LPS2 may be used with the timestamps to calculate axle speed as the distance over the time difference. Figure 3.5 illustrates this output table for the truck pass described above. While it may seem overly precise to compute speed per axle, it ensures the data processing scheme can handle situations where a truck may change speed while passing through the gauge array.

W30: Axle Speed

1: Axle	2: Speed,mph
1.000000	40.705563
2.000000	40.404040
3.000000	40.106952
4.000000	40.705563

Figure 3.5: Sample Truck Pass Axle Speed in DADiSP.

3.4 AXLE SPACING COMPUTATIONS

In order for the processing scheme to classify axles by type (i.e., single, tandem, tridem, etc.), the axle spacing must first be determined. In this step, the axle speeds from the previous computation are used in conjunction with the timestamps from LPS1 to determine spacing between axles. In this case, distance between axles is calculated as the average axle velocity from two consecutive axles multiplied by the time difference between those consecutive axles. Figure 3.6 shows computed axle spacing for the sample truck pass described above.

W31: Axle Spacing

1: Axle	2: Distance from previous, in.
1.000000	0.000000
2.000000	158.455721
3.000000	217.508497
4.000000	34.135206

Figure 3.6: Sample Truck Pass Axle Spacing in DADiSP.

3.5 AXLE CLASSIFICATION

The axle spacing data generated in the previous step are used to classify the axle group type. By default, the first truck axle is always designated as the steer axle and given an axle code of 1.1.

Consecutive spacings are then evaluated to group axles into single, tandem, tridem, etc. groupings. A 54 inch critical spacing is used to group axles together into a single group. Figure 3.7 shows the axle groupings for the sample truck. Consistent with Figure 3.3, this truck consists of a steer axle, a drive single axle followed by a rear tandem axle group.

W34: Axle Types

1: Axle	2: Axle Type
1.000000	1.100000
2.000000	1.000000
3.000000	2.000000
4.000000	2.000000

Figure 3.7: Sample Truck Pass Axle Classification in DADiSP.

3.6 CALCULATE LATERAL OFFSET FROM EDGE STRIPE

The lateral offset from the edge stripe is calculated from the LPS timestamp data and axle speeds computed above. Figure 3.8 illustrates the key parameters and equation used to find the offset as previously documented *(Timm and Priest 2004)*. In the figure, t_1, t_2 and t_3 are the timestamps corresponding to those shown above in Figure 3.4 and the $x/(t_3-t_1)$ computation in the equation corresponds to the velocity computation shown in Figure 3.5. Figure 3.9 shows example data for the truck pass described above. Note that the data appear reasonable as the steer axle (single tire) is furthest from the edge stripe while the other tires are closer to the stripe.

$$y' = (\tan\alpha)\cdot\left[\frac{x}{t_3 - t_1}\cdot(t_2 - t_1) - f\right]$$

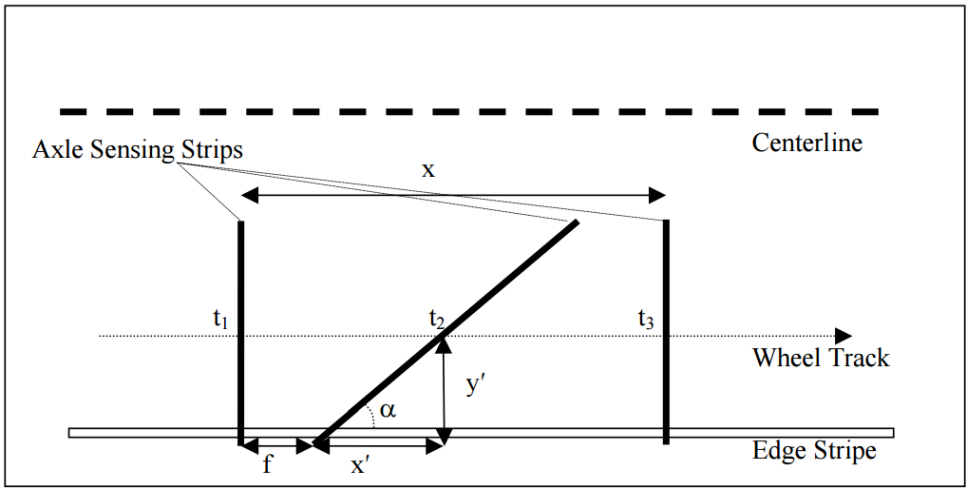

Figure 3.8: Lateral Offset Computation Schematic *(Timm and Priest 2004).*

W32: Axle Offset

1: Axle	2: Offset, in.
1.000000	32.348657
2.000000	26.588444
3.000000	14.588235
4.000000	15.842388

Figure 3.9: Sample Truck Pass Lateral Offset in DADiSP.

3.7 FIND STRAIN GAUGE PEAKS

The next step in the process is to systematically search each of the strain gauge signals looking for maximum tensile or compressive responses as illustrated in Figure 3.10. In this example, the relatively smooth strain trace clearly shows each axle and the superimposed straight lines identify the peak response from each axle. While visually a straightforward concept, the algorithm is somewhat complex in that it uses the known axle speed (Figure 3.5) and known distance between the LPS1 sensor and each strain gauge to estimate when the peak should have occurred (time = distance/velocity). The algorithm uses this estimate to establish a small window of time over which to search for the maximum response. This allows for some uncertainty in when the maximum occurred due to slight variations in speed, etc. The time stamps of the peak, and corresponding peak voltages, are then recorded and plotted with the strain signal as shown in Figure 3.10. Plotting the data in this fashion allows the user to quickly inspect the data for quality and ensure that all peaks were properly captured.

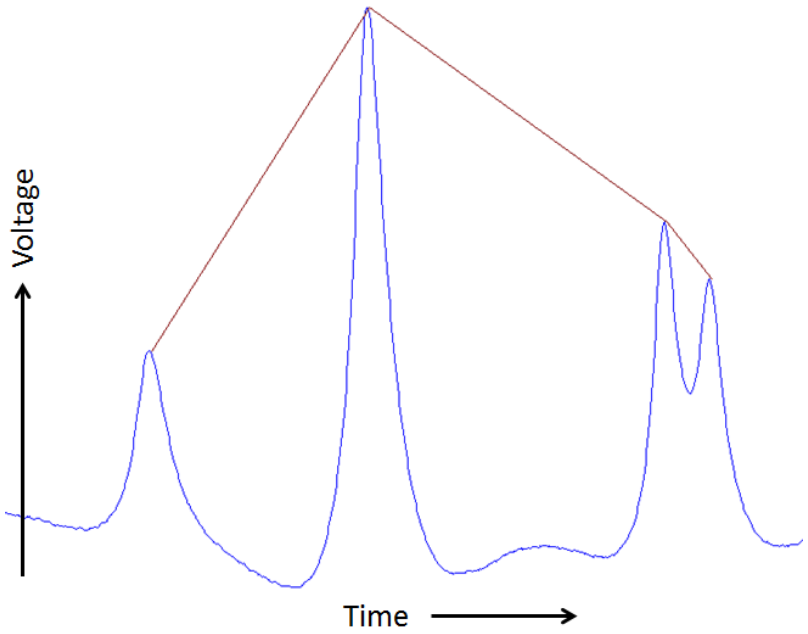

Figure 3.10: Sample Strain Gauge Trace and Peak Values in DADiSP.

3.8 TABULATE SUMMARY OUTPUT DATA

All of the steps described above happen automatically when the user clicks the data processing button within DADiSP. The final step is to compile all the data into a single table that may be output to Excel, Access or any other program. The final step also includes multiplying the raw voltage output by corresponding gauge factors that converts signal voltage to microstrain. In examining the data provided by ODOT, gauge factors for the Dever-Conner site were well documented and easily incorporated into the Dever-Conner template. The Medford site had gauge factors specified, but the excitation voltage used at that site was not documented and an assumption was made to in order to use those gauge factors. No gauge factors were found for the Redmond site in the original files obtained from ODOT. Further inquiries to ODOT did not result in Redmond gauge factors. It is possible that they may be obtained in the future, but at this time, provisional gauge factors are in use based on known excitation voltage and gauge factors from the Dever-Conner site.

The output table is much too large to include in this document, but it includes the following output columns listed below. The number of ASG columns in the summary output table correspond to the number of gauges in the data file. The last two items, maximum longitudinal and maximum transverse microstrain, are found by obtaining the maximum response from the respective subset of gauges for each axle pass. These columns may be considered the “best hit” responses in the longitudinal and transverse directions.

- Truck ID (user entered)
- Axle number

- Speed of axle, mph
- Axle offset, in.
- Distance from previous axle, in.
- Axle type
- ASG baseline microstrain
- ASG peak time, sec
- ASG peak microstrain
- ASG strain magnitude (ASG peak – ASG baseline)
- Maximum longitudinal microstrain
- Maximum transverse microstrain

4.0 SITE-SPECIFIC DATA AVAILABILITY AND PROCESSING SCHEMES

As described above, each test site was unique in terms of data format, organization, etc. The following subsections detail the data availability and present the processing template from each site.

4.1 REDMOND US 97

Data were collected on thirteen test dates between September 25, 2008 and November 17, 2009. The data were found in three different formats that included text files, Excel spreadsheets and TDMS files. Though each format works with the DADiSP template created for this site, some pre-DADiSP work is needed prior to entering into DADiSP. The text files require a timestamp column to be created while the TDMS files require a TDM file importer available from National Instruments to open the file in Excel which allows the user to copy and paste the raw data into DADiSP.

Figure 4.1 shows the Redmond processing template created in DADiSP. The table on the left side allows the user to paste in raw data. The highlighted button at the top is then used to initiate the automated processing algorithms at which point the program asks for the truck identification number from the user. After entering a truck number, the program follows the procedural steps described in Section 3.1. The strain traces are plotted along with the selected peak values as shown in the nine graphical windows of Figure 4.1 while the output data are tabulated on the right side of the figure. These steps are accomplished almost instantaneously. The graphical strain trace windows are arranged to resemble the actual field arrangement of gauges shown in Figure 3.1a. For example, the center row of plots corresponds to the center-of-wheelpath gauges while the upper row is left of wheelpath and the lower row is right of wheelpath near the edge stripe. The first column of plots are the first set of longitudinal gauges as traffic moves left-to-right, followed by the transverse gauges in column two and finally the second set of longitudinal gauges. This arrangement allows for intuitive and rapid inspection of the data.

While there are a large number of data files available for processing, there are some limitations worth noting regarding this test site. First, the gauge factors are currently based on an assumed excitation voltage. The assumed value was based on the documented value from the Dever-Conner site. To be fully confident in the data, this value must be confirmed. Second, in reviewing the data files, it was noticed that some raw data files contained more than just a single truck. Some included what appeared to be an additional axle or two of the following truck. This was presumed to have resulted from triggering on data storage on for a particular truck and not turning it off in time. Further refinement of the data processing scheme may be needed that allows the user to focus on the target truck in each data file. Third, there appeared to be a significant number of 2-axle vehicles collected. Until the data are fully processed, it is not known the significance of these vehicles in terms of pavement strain levels.

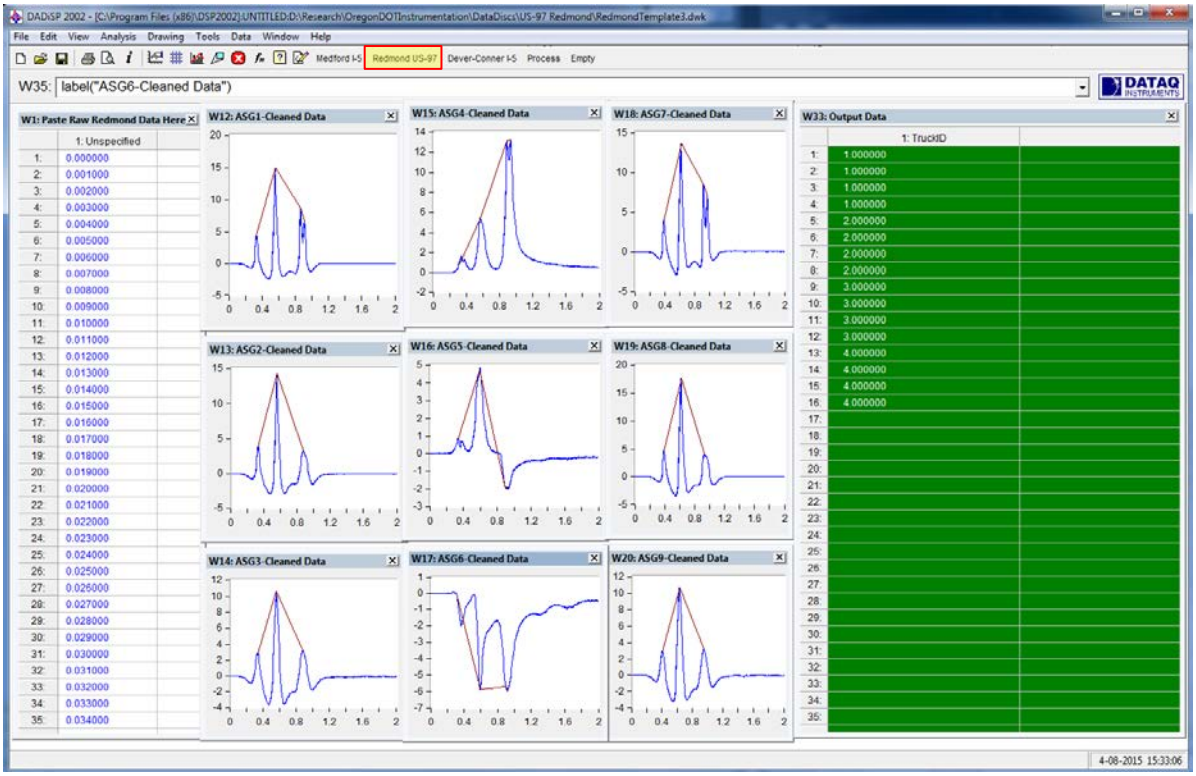

Figure 4.1: Redmond US 97 DADiSP Processing Template.

4.2 MEDFORD I-5

The Medford files included only one testing date which had 724 individual files representing 724 truck events. The data files are in TDMS format which requires the National Instruments TDM file importer. Figure 4.2 shows the Medford processing template, which has the same general layout as the Redmond template because the same gauge arrangement was used in both locations. In this case, the user would follow the same procedure as above, but instead click on the highlighted Medford I-5 button to execute the processing algorithms. Note that ASG3 (bottom left strain trace) appears extremely noisy. This gauge appears to be non-functional. The processing algorithms still look for and record peak values, but the maximum functions which survey all the longitudinal and transverse gauges would essentially ignore this gauge since the strain values are so low.

The Medford site is somewhat limited in that only one day was devoted to data collection. While there are a large number of vehicle events from that one date which should enable some useful information to be gathered, it appears that many of the files correspond to two-axle vehicles (light duty trucks or passenger cars). Also, similar to the Redmond site, it appears that some of the files contain more than a single truck which will require further refinement of the processing algorithms. Despite these issues, the biggest concern with the Medford site is the current lack of strain gauge calibration factors which forces the processing template to use representative values based on the other test sites.

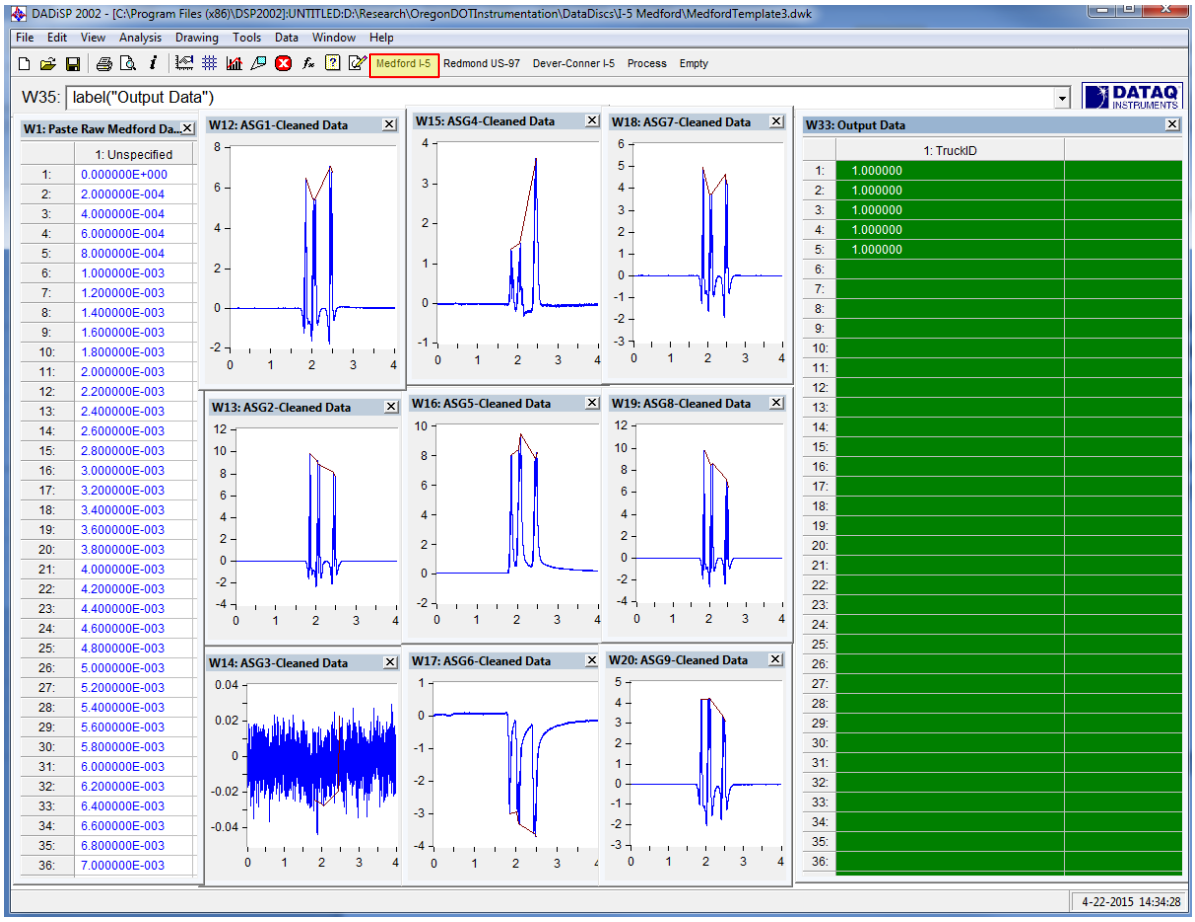

Figure 4.2: Medford I-5 DADiSP Processing Template.

4.3 DEVER-CONNER I-5

Dever-Conner was the most complex test site for a number of reasons. First, it featured two strain gauge arrays consisting of 12 ASGs with the axle sensing strips between them, as shown in Figure 3.1b. The first array was placed on an aggregate base (AB) layer while the second array was on a rubblized base (RB) layer. Second, this test site had the most data collection dates of the three with 17 dates from June 20, 2006 through November 19, 2009. Third, and perhaps most critically, it appears that the data collection efforts changed over time resulting in 11 different file formats for this one test site. This means that 11 different data processing templates will need to be developed for this site. Furthermore, on some test dates, the files appear to have gauges out of order, missing some gauges, etc. These problems are listed in Table 4.1 according to the 11 different file formats. An ideal file format for Dever-Conner would contain time, LPS sensor data, 12 ASG signals on the aggregate base followed by 12 ASG signals on the rubblized base. Unfortunately, as noted in the table. This was not achieved on any of the test dates.

Table 4.1: Dever-Conner File Format Issues

Format	Dates	Major Issues	Comments
1	6/20/2006 6/7/2007 9/4/2007	No LPS sensor data. No time stamps given.	Lacking LPS data, entirely new processing scheme will be required.
2	1/23/2008	No LPS sensor data. Time given in odd format (time + milliseconds).	
3	9/23/2008	Only 10 channels in data file. No labels provided.	Significant effort will be required to sort out this format. Raw data will have to be investigated to determine which channel corresponds to which gauge. A processing scheme will then be developed based on the findings.
4	10/29/2008 12/4/2008 1/9/2009 2/20/2009	Only 12 ASG channels in data file. They are presumably the AB gauges, but will need to be confirmed.	These test dates will only provide strain data from the aggregate base section.
5	3/13/2009	Only 12 ASG channels in data file. The last two gauges are out of order (ASG 12 comes before ASG 11). Gauges are labeled as "sg".	Further investigation needed to determine if gauges out of order was typo, or physically wired into data acquisition system that way. Will also need to investigate if these are the AB or RB gauges.
6	5/6/2009	All 12 AB strain gauges listed, but only 9 RB listed. Also, numbering of RB skips (missing RB2, RB8, RB10)	Raw data will have to be investigated to determine/verify which gauges were active.
7	6/10/2009	Only 11 AB gauges listed as active (missing AB2). AB12 is listed with the RB gauges. Only 9 RB gauges listed.	
8	7/14/2009	Only 11 AB gauges listed as active (missing AB2). Only 9 RB gauges listed.	
9*	8/19/2009	Only 9 RB gauges listed.	This is the "best" date available. It does not contain all the available ASG's, but it does have them listed in order which was validated by examining raw data.

Format	Dates	Major Issues	**Comments**
10	9/22/2009 11/19/2009	Only 11 AB gauges listed. AB12 listed amongst RB gauges. AB2 missing. Only 10 RB gauges listed. RB1 listed with AB.	Raw data will have to be investigated to determine/verify which gauges were active.
11	10/28/2009	Only 11 AB gauges listed. AB12 listed amongst RB gauges. AB2 missing. Only 10 RB gauges listed. RB1 listed with AB, RB10 missing, but RB11 included.	

**This file format used to create first Dever-Conner processing template.*

Since the purpose of Phase I of this project was to catalogue and assess the current state of the data and establish rudimentary processing schemes for the three sites, it was decided not to develop all 11 schemes needed for the Dever-Conner site. This was beyond the original understanding and constraints of the project. Given the 11 formats listed in Table 1, it was decided to develop the Dever-Conner scheme for format #9 as it had the least number of major issues. Given the large number of issues with other formats, the data were thoroughly investigated prior to developing the scheme to be sure gauge labels matched the gauges correctly. Fortunately, this was the case.

Figure 4.3 illustrates the Dever-Conner processing template corresponding to format #9. The layout is similar to that of the previous two sites. The raw data are copied into the template on the left-hand side while the outputs are tabulated on the right-hand side. The 21 graphical windows in the middle correspond to the 12 AB strain gauges and the 9 RB strain gauges, respectively. In this case, the graphical windows are arranged such that the middle column corresponds to the center of the wheelpath and traffic moves from top to bottom through the gauge arrays. The top four rows of windows represent the AB gauges and the bottom 3 correspond to the first 9 RB strain gauges (3 longitudinal and 6 transverse gauges). Like the other templates, after loading raw data, the user simply clicks the Dever-Conner I-5 button, enters a truck number and watches while the processing algorithms quickly plot the gathered peak data and tabulate the outputs.

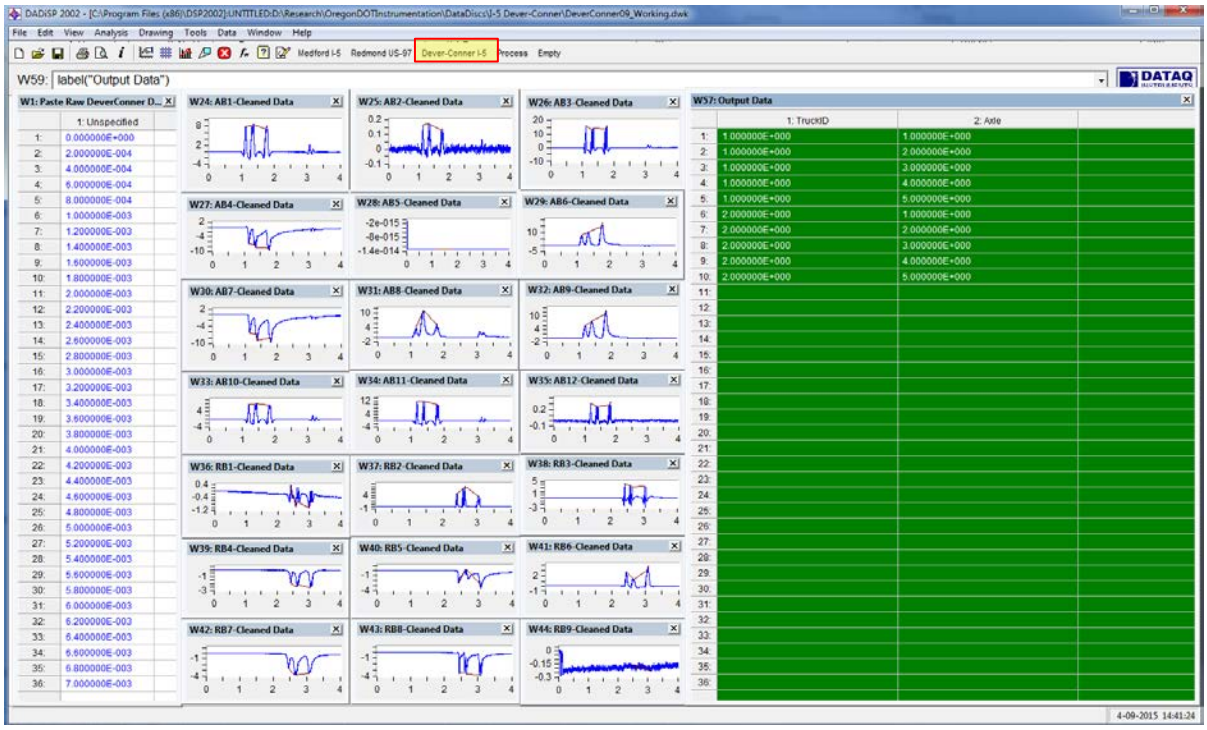

Figure 4.3: Dever-Conner I-5 DADiSP Processing Template.

Dever-Conner's large number of data collection dates, and two pavement sections, creates great potential for producing valuable pavement response information. On any given date, direct comparisons may be made between the aggregate base and rubblized base section. Furthermore, pavement responses over time may be determined and compared between the two sections. The greatest limitation, as demonstrated Table 1, is that significant effort will need to be expended to extract all the data.

5.0 PRELIMINARY MODEL EVALUATION WITH MEASURED DATA

The other major task within Phase I was to perform mechanistic simulations of each of the three test sections to compare theoretical and measured pavement responses. The layered elastic computer program, WESLEA for Windows, was used for this purpose. WESLEA was selected for this project because it is capable of simulating various loading configurations (axle types) on customizable pavement layers. The following subsections discuss the inputs used in the theoretical strain predictions (i.e., pavement structure, material properties and WIM data), present the strain comparisons for each site and introduce some further analysis that was conducted.

5.1 PAVEMENT STRUCTURE

The pavement cross section for each site is shown in Figure 5.1. The layer type and thicknesses were obtained from construction plans provided by ODOT. The construction plans for each section were similar to the plan shown in Figure 5.2 from the Redmond site. It is important to note that the exact pavement depths at the instrumentation site may not be precisely known. This was due to estimating the mile point of the instrumentation location and using the plan sheet representing the nearest station. For WESLEA simulation, the AC layers were grouped together as shown in Figure 5.3 and were input into WESLEA as shown in Figure 5.4 for the Redmond site.

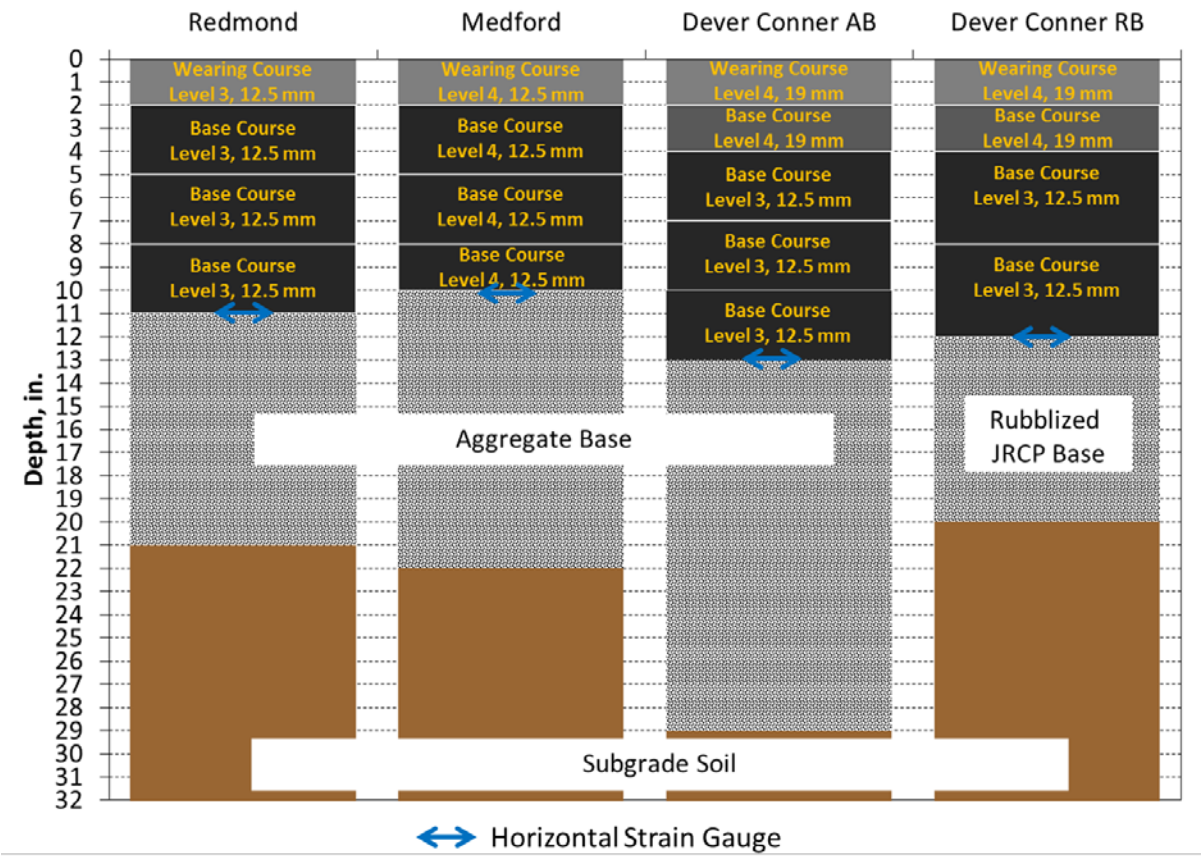

Figure 5.1: Pavement Cross Sections.

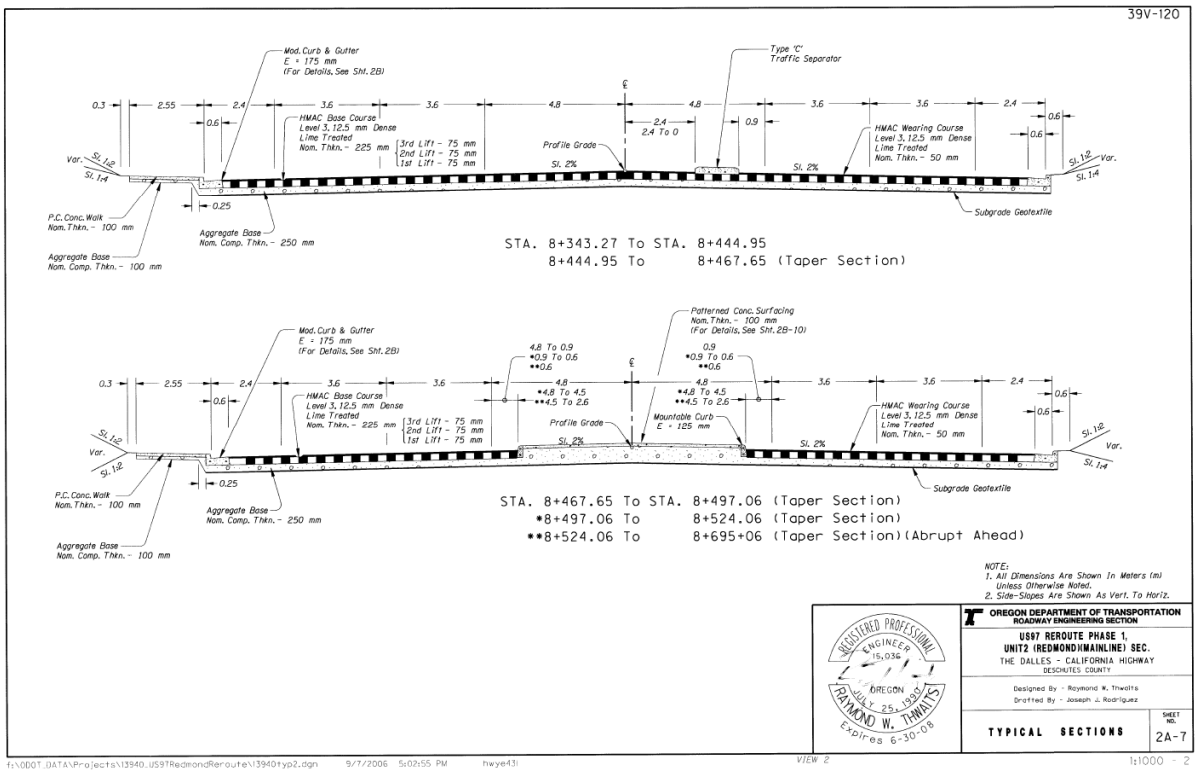

Figure 5.2: Redmond Construction Plan.

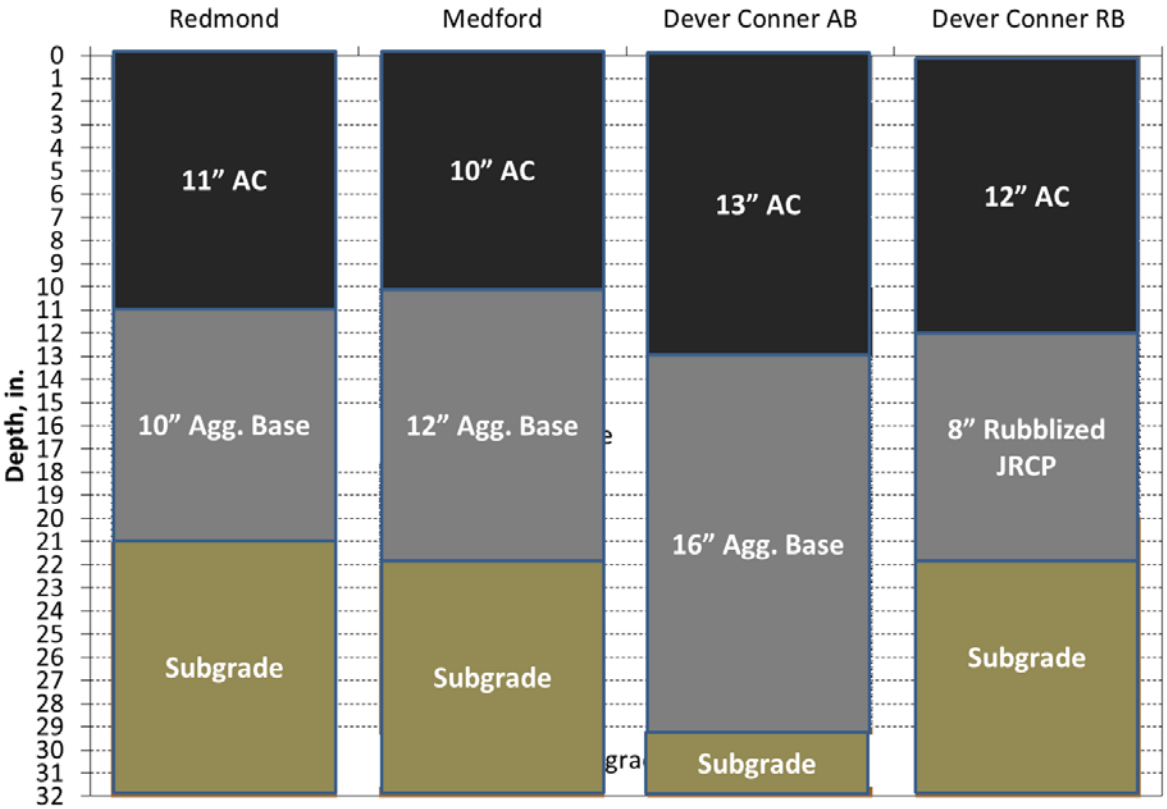

Figure 5.3: Layer Groupings for WESLEA Structural Inputs.

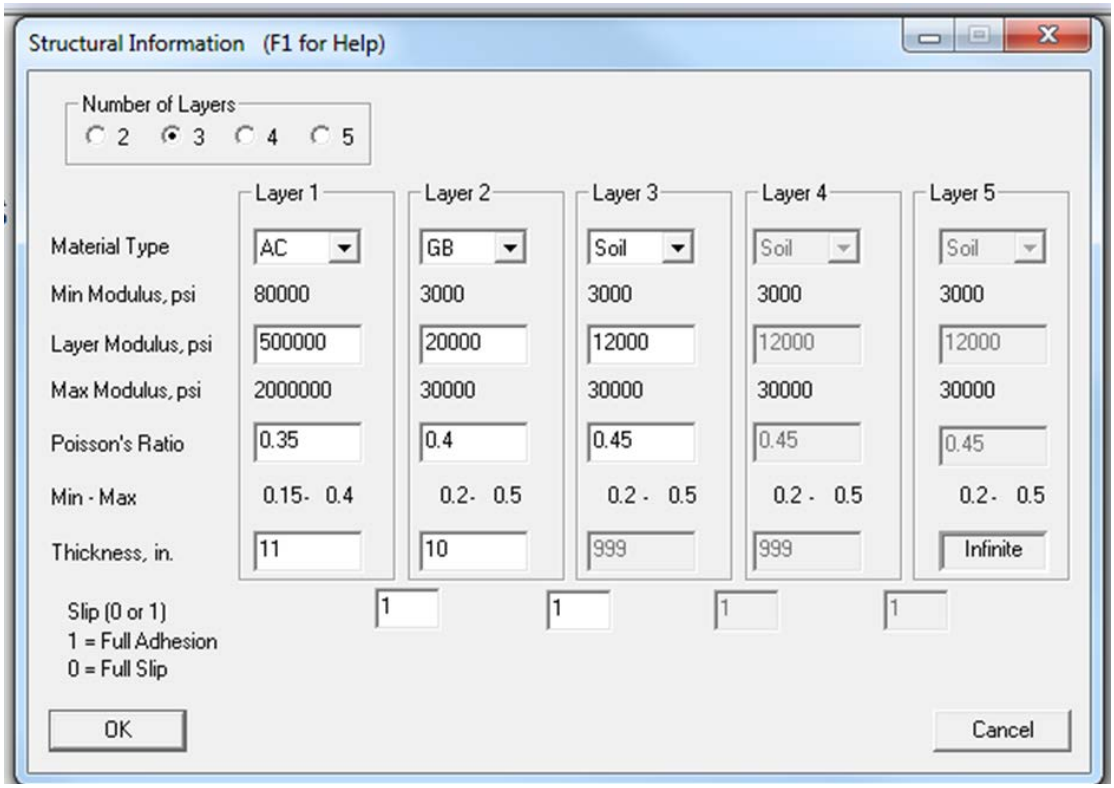

Figure 5.4: WESLEA Structural Input Screen.

5.2 MATERIAL PROPERTIES

It can also be seen in Figure 5.4 that the layer modulus and Poisson's ratio are required inputs. WESLEA defaults were used for these values because exact material properties were not available. However, reasonable agreement was found when the WESLEA default values were compared to modulus values backcalculated from falling weight deflectometer (FWD) testing that was provided by ODOT. The original intention of the FWD testing was strain gauge verification. However this information was utilized to provide an estimate of the in-place material properties. Figure 5.5 shows the backcalculated AC modulus at three drop load levels from FWD testing at the Redmond site on May 22, 2009. It can be seen that the backcalculated modulus values range from approximately 450 ksi to 700 ksi. The average of the backcalculated AC modulus was 540 ksi. Average backcalculated modulus values were also found for the base and subgrade layers and are presented in Table 5.1 with the WESLEA default values used for each layer. Even though the match is not exact (the default AC and base moduli are slightly lower than the backcalculated and the default subgrade modulus is slightly higher), it was determined that the WESLEA default values were in reasonable agreement with the backcalculated values. Lacking more precise testing data, this was deemed sufficient for the purposes of simulation.

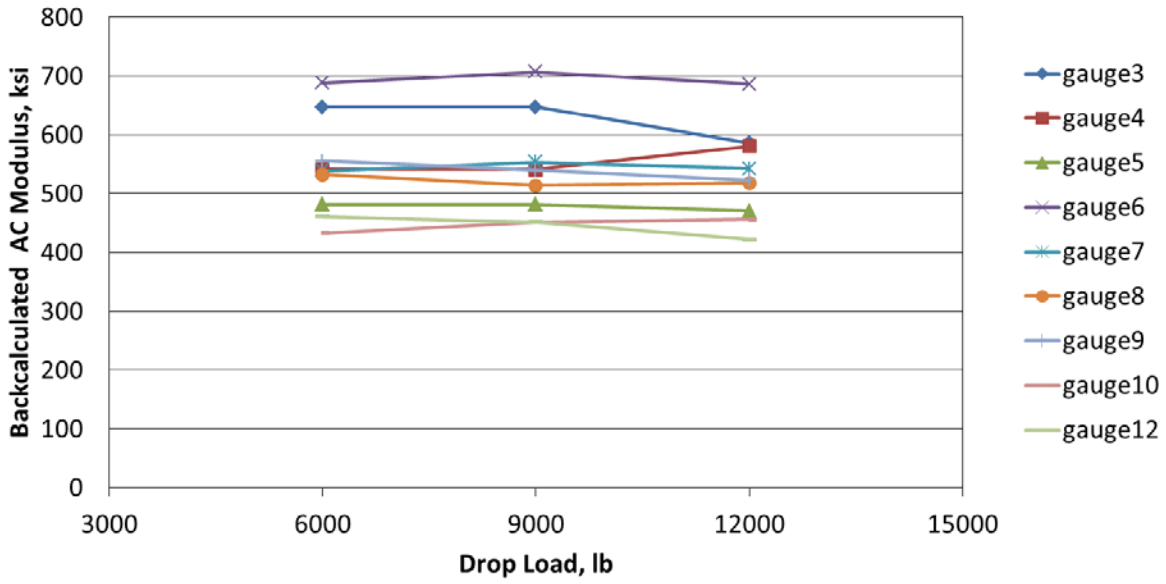

Figure 5.5: May 22, 2009 Redmond FWD Results.

Table 5.1: Redmond FWD Results and WESLEA Default Moduli

	Modulus, ksi				
Drop Load, lb	**6,000**	**9,000**	**12,000**	**Average**	**WESLEA Default**
HMA	542	543	532	539	500
Aggregate Base	23.3	32.7	37.5	31.2	20.0
Subgrade	9.8	9.6	10.1	9.8	12.0

5.3 AXLE LOADING AND WIM DATA

As mentioned in Section 2, WIM data were provided in the original data transfer to NCAT. Though WIM files were available, only in a few cases was it possible to link WIM events to strain events since they were collected and stored by separate systems. In other words, the exact weight of a given vehicle (measured by the WIM) could not be directly linked to its corresponding pavement response (measured by the gauge array) for every load event. Often, the WIM files and strain values were not taken over the same time period. For example, at the Medford site on November 24, 2009 WIM data were collected from around 11:00 am to 4:30 pm with a total of 837 WIM events. At this same location and date, the corresponding strain files were collected from 3:30 pm to 5:15 pm with a total of 724 strain events.

It should be mentioned that it is possible to link the WIM and strain responses on a vehicle-by-vehicle basis at the Dever-Conner site on June 7, 2007 because on this date a list was manually taken in the field to link WIM and strain events. However, this analysis was not undertaken in this phase in the project due to the challenges of the fluctuating file formats discussed previously

but it can be used in Phase II of this project to validate the analysis done when a direct link was unavailable.

Statistical techniques were used to circumvent the inability to match WIM data and strain events. Table 5.2 summarizes the WIM vehicles captured at the Medford site on November 24, 2009. It can be seen that the vast majority of vehicles with more than 3 axles were 5 axle trucks. The individual axle weights of the 5 axle trucks are examined in Table 5.3 where the 90^{th}, 50^{th} and 10^{th} percentile axle weights are shown for each section. The maximum axle weight for steer and tandem axles, at each percentile, was determined and used as the loading input for the WESLEA simulations.

Each location, axle type and load percentile was input into WESLEA for simulation and the results were output to Excel. The WESLEA outputs of interest, longitudinal microstrain as a function of distance, were then copied into another workbook for comparison with measured data. Figures 5.6 and 5.7, which will be used in the following section for further comparisons, show the theoretical strain generated under the 50^{th} percentile steer and tandem axles at the Redmond site.

Table 5.2: Medford WIM Summary from November 24, 2009

Number of Axles	Number of Trucks	Percent of Total
2	400	48%
3	42	5%
4	54	6%
5	298	36%
6	7	1%
7	14	2%
8	4	0%
9	5	1%
10	2	0%
11	1	0%
12	1	0%
13	9	1%
14	0	0%
Total	837	100%

Table 5.3: Summary of WIM Data and WESLEA Inputs

Location / Date	Percentile	Weight, 1,000 lbs						
		WIM Data					WESLEA Inputs	
		Axle 1	Axle 2	Axle 3	Axle 4	Axle 5	Steer	Tandem
Redmond 4/22/2009	10th	9.2	9.8	9.8	9.5	9.0	9.2	9.8
	50th	11.0	13.3	13.1	14.0	13.8	11.0	14.0
	90th	12.6	17.1	17.2	16.1	16.8	12.6	17.2
Medford 11/24/2009	10th	7.2	8.7	8.3	7.1	7.4	7.2	8.7
	50th	8.6	12.8	12.3	13.0	12.7	8.6	13.0
	90th	10.1	16.7	16.7	16.5	16.4	10.1	16.7
Dever - Conner 8/19/2009	10th	9.4	9.4	8.7	7.1	6.8	9.4	9.4
	50th	10.9	13.3	13.3	11.1	12.0	10.9	13.3
	90th	12.0	20.1	19.7	20.5	20.4	12.0	20.5

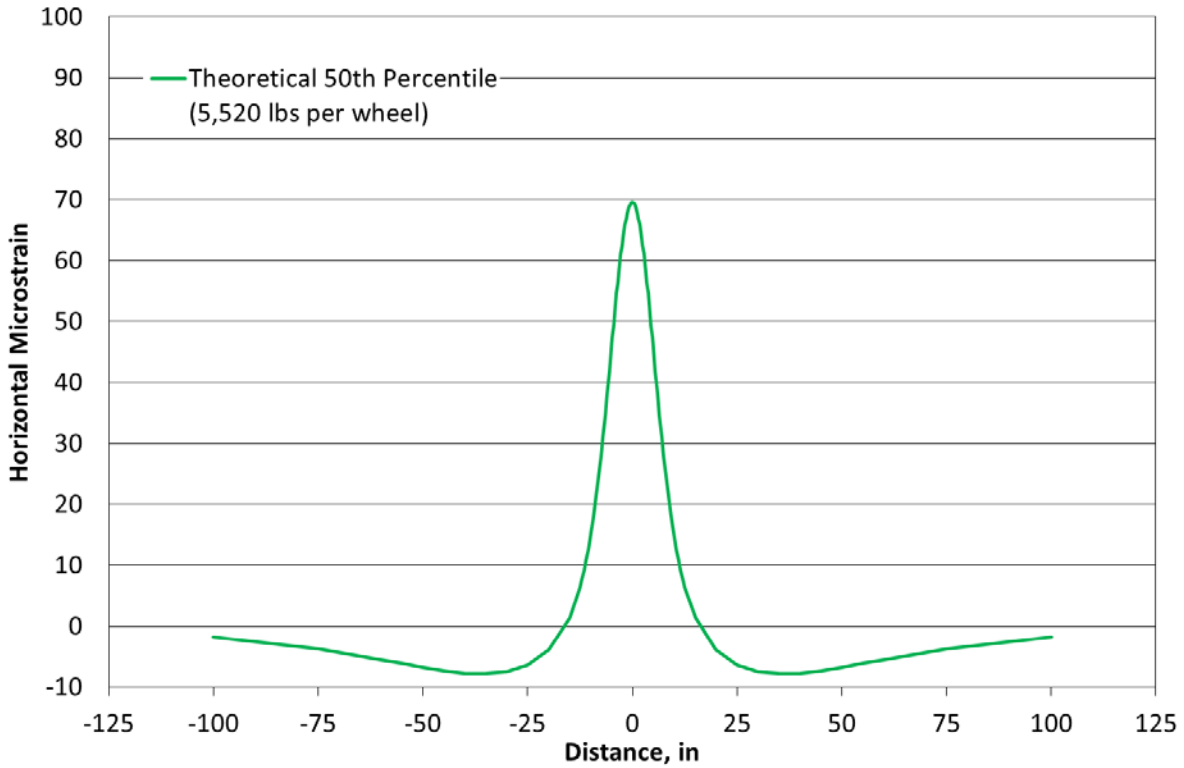

Figure 5.6: WESLEA Theoretical Strain for Redmond 50th Percentile Steer Axles.

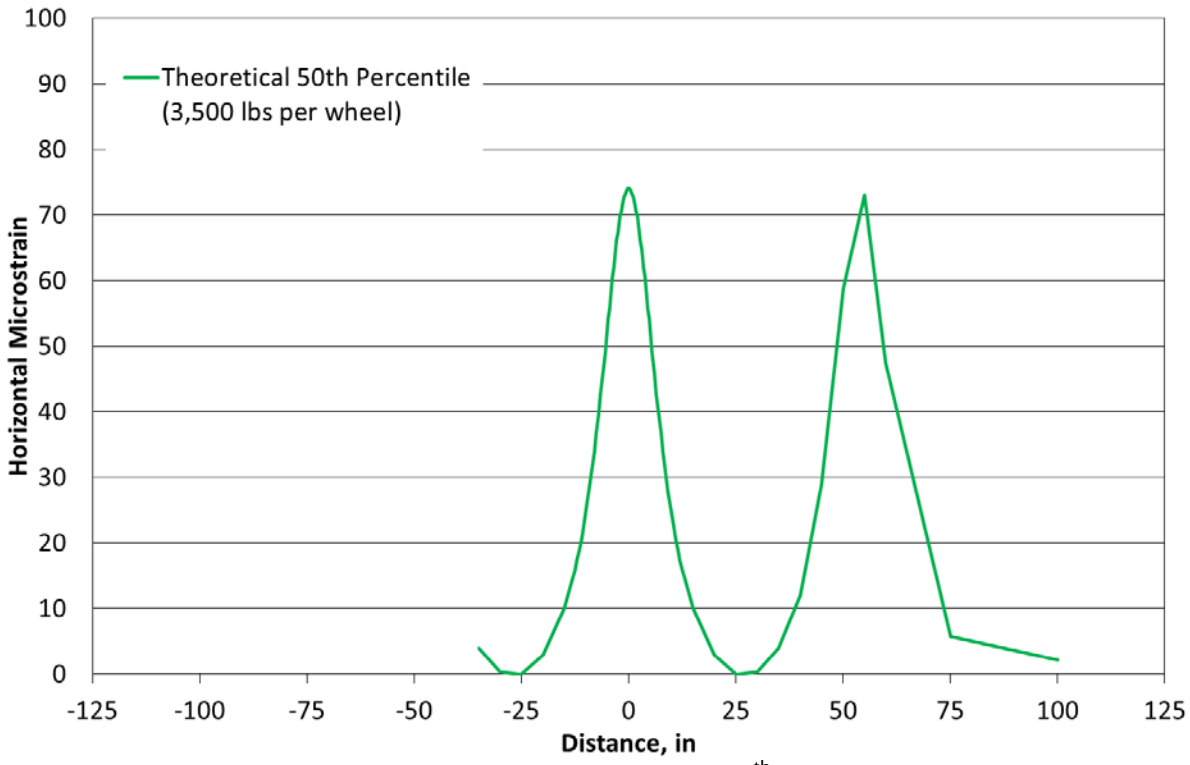

Figure 5.7: WESLEA Theoretical Strain for Redmond 50th Percentile Tandem Axles.

5.4 MEASURED STRAIN FOR COMPARISON

The raw strain files and the processed data from DADiSP, discussed previously, were used to develop the measured responses for the comparison. From the plot of raw voltage versus time in Figure 5.8, a particular gauge and timeframe was selected for further analysis. For this particular example, a steer axle was selected. Gauge SG10 was then found to have the highest response and the timeframe of interest was 0.35 to 0.65 seconds. A table with the maximum, minimum, and the difference between the maximum and minimum was also used with Figure 5.8 in the spreadsheet to determine which gauge captured the greatest pavement response.

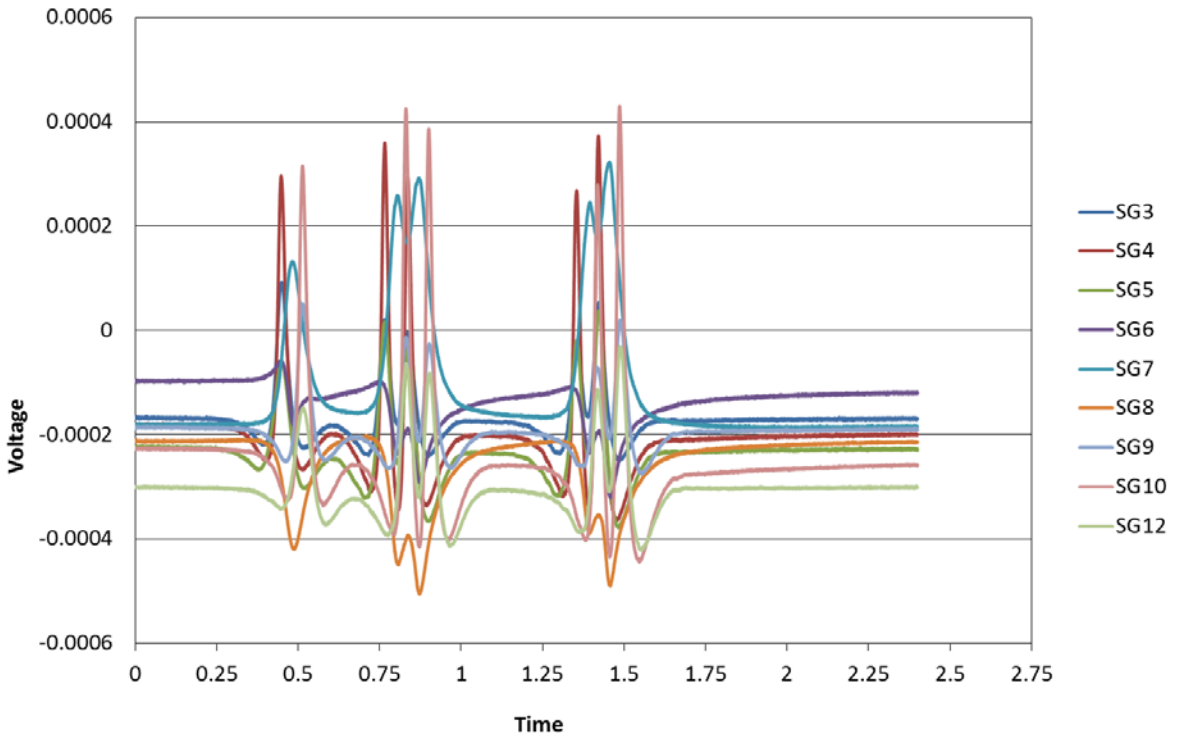

Figure 5.8: Raw Voltage used for Measured Response.

After selecting the gauge and timeframe of interest, the raw voltage was converted to strain (using the appropriate gauge factor, if available) and the time was converted to distance using the speed calculated from DADiSP in the processed data. The measured strains responses were then plotted with the theoretical strains from Figures 5.6 and 5.7. It can be seen in Figures 5.9 and 5.10 that the measured strains follow the same trend as a function of distance as the theoretical strains, but the magnitudes were somewhat different. This may be due to several factors. First, since the weight of the axle that created the measured response is unknown, a perfect match between measured and predicted may not be expected due to loading variance between measured and modeled. Second, representative material properties were used. More accurate material properties may provide a closer match between measured and predicted responses.

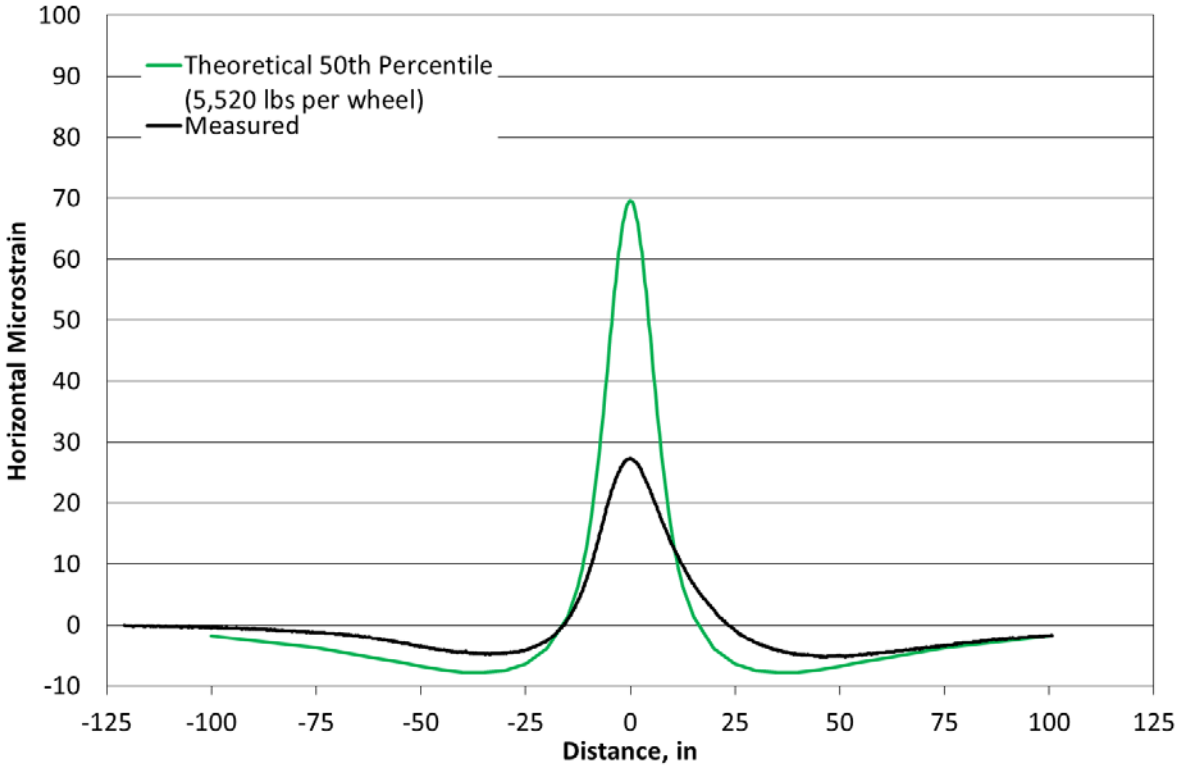

Figure 5.9: Redmond Measured and Predicted Strain Comparison for Steer Axles.

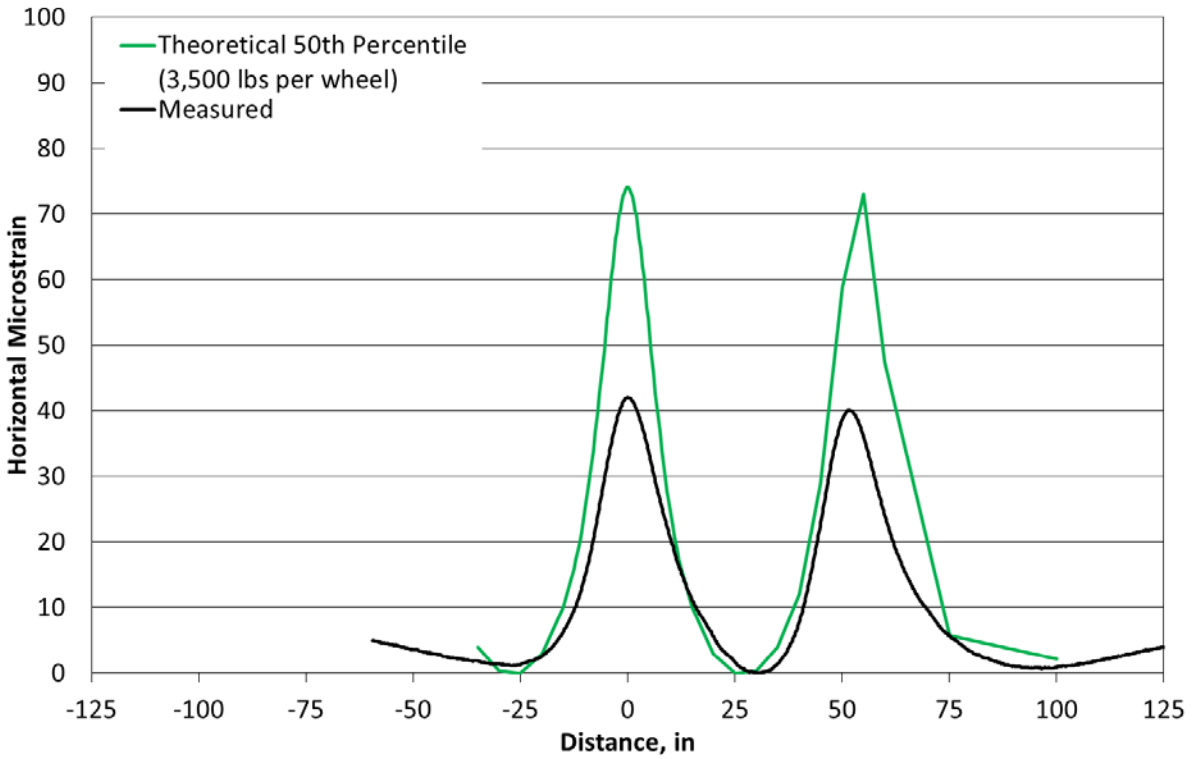

Figure 5.10: Redmond Measured and Predicted Strain Comparison for Tandem Axles.

5.5 STRAIN COMPARISONS

Following the procedure described above, the 90th, 50th and 10th percentile steer and tandem axle loads were compared to measured strain responses from multiple 5 axle vehicles chosen randomly within the files for each site. The theoretical strains at the Redmond site are compared with strains measured from two different 5 axle vehicles (collected on April 9, 2009) in Figures 5.11 through 5.14. Figures 5.11 and 5.12 compare the theoretical strain levels under the steer axles and Figures 5.13 and 5.14 compare the tandem axles at the Redmond site. Tandem axles from the Medford site (collected on November 29, 2009) are compared in Figures 5.15 and 5.16.

Dever-Conner strain comparisons are shown in Figures 5.17 through 5.22 for the 90th, 50th and 10th percentile steer and tandem axle loads. The plots for each percentile at the Dever-Conner site have been separated so the impact of base type can be seen. In all the plots there was a reduction in both the theoretical and measured strain levels from the aggregate base to the rubblized base. However, the reduction in measured strain appears to be greater than the theoretical strain reduction.

In all cases the theoretical strain levels were found to be greater than the predicted strain levels. As discussed previously, this discrepancy is a result of numerous factors ranging from WESLEA inputs to voltage conversions. The comparison can be improved with more accurate inputs and the creation of a response and WIM database that allows, for example, the 90th percentile strain event to be compared with the 90th percentile load event.

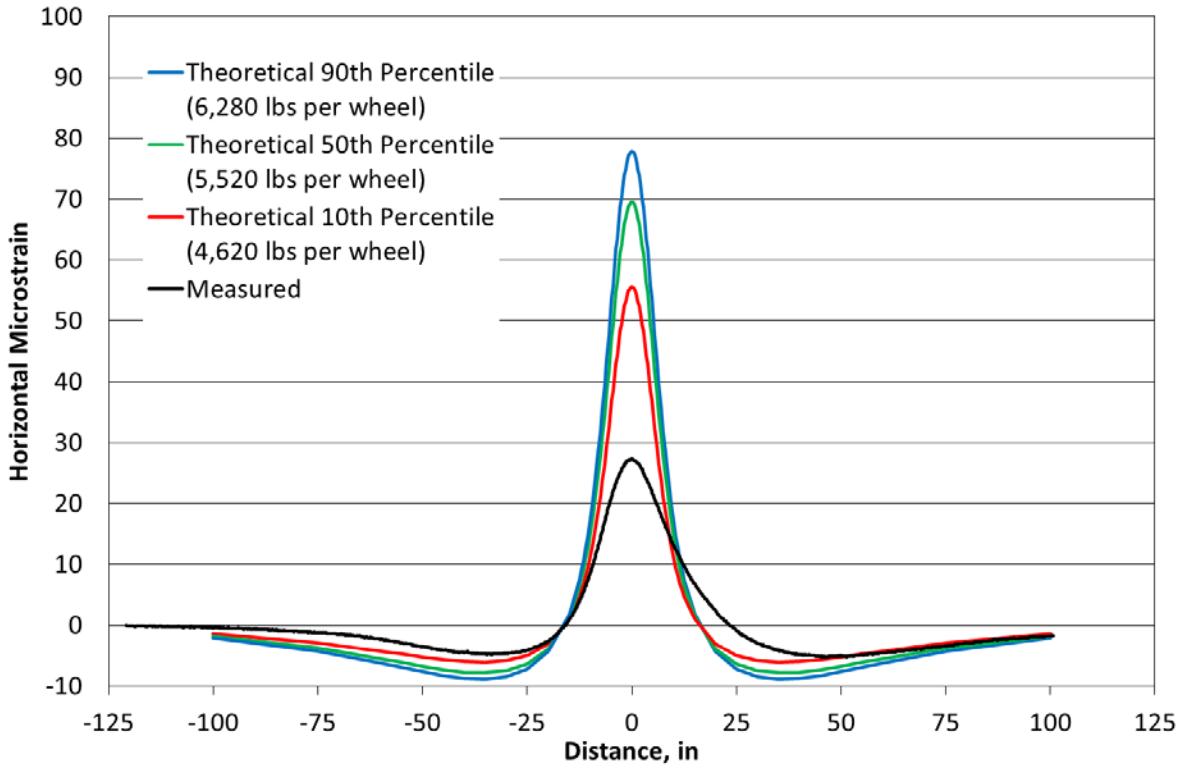

Figure 5.11: Redmond Steer Axle Strain Comparison #1.

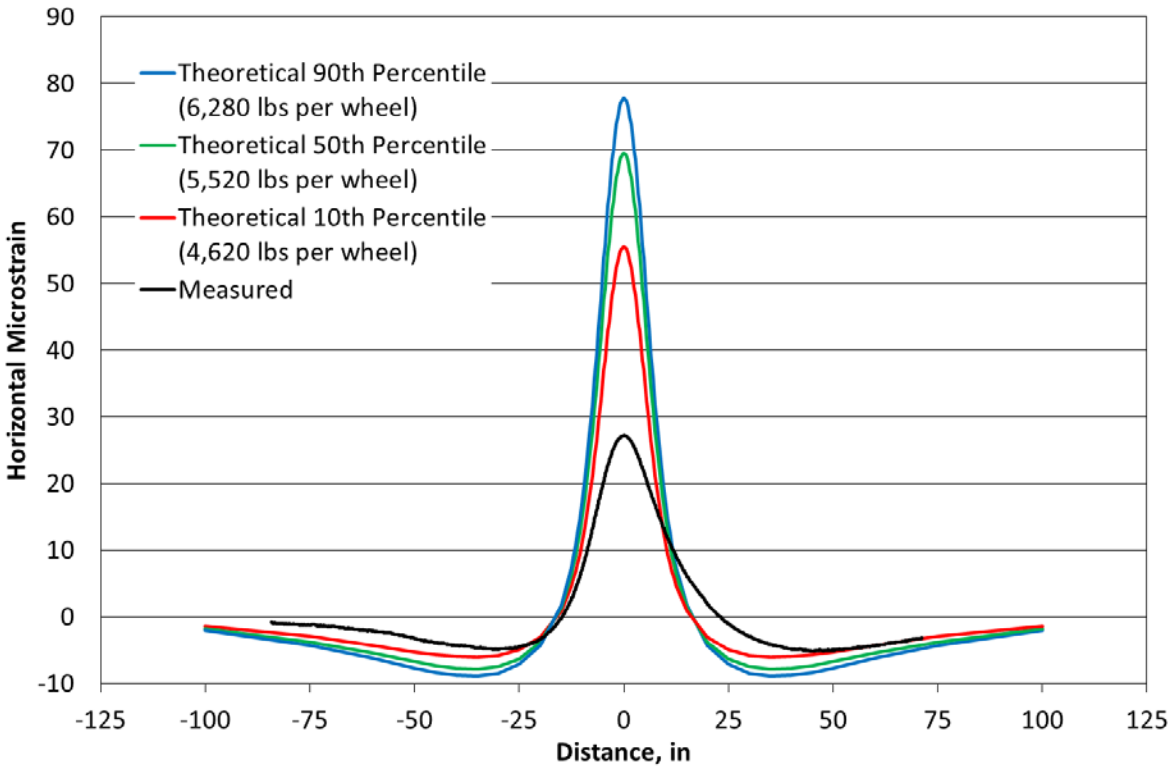

Figure 5.12: Redmond Steer Axle Strain Comparison #2.

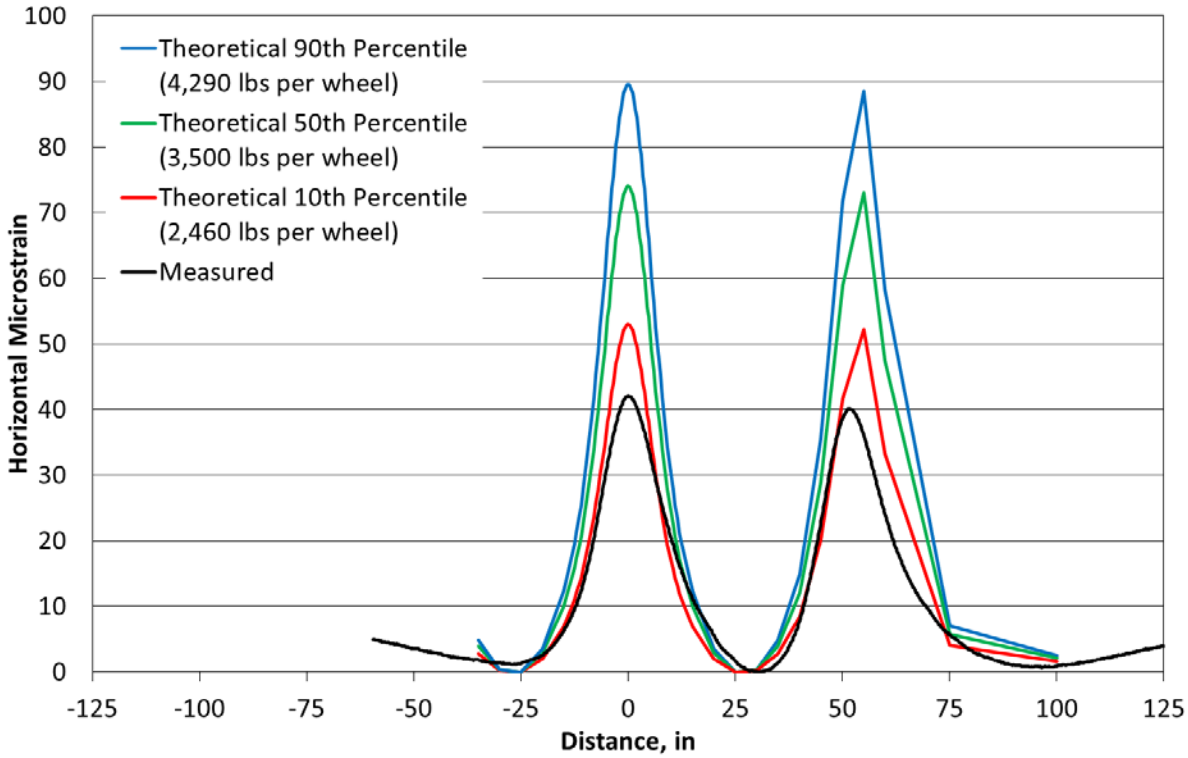

Figure 5.13: Redmond Tandem Axle Strain Comparison #1.

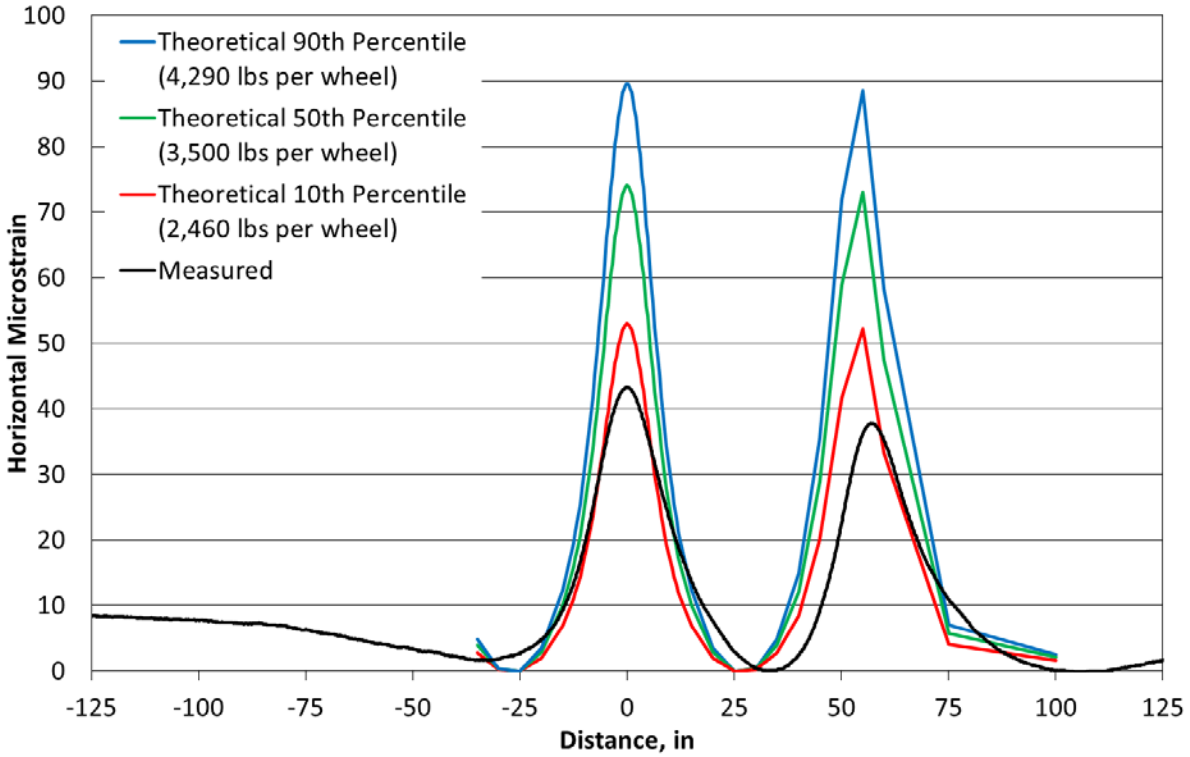

Figure 5.14: Redmond Tandem Axle Strain Comparison #2.

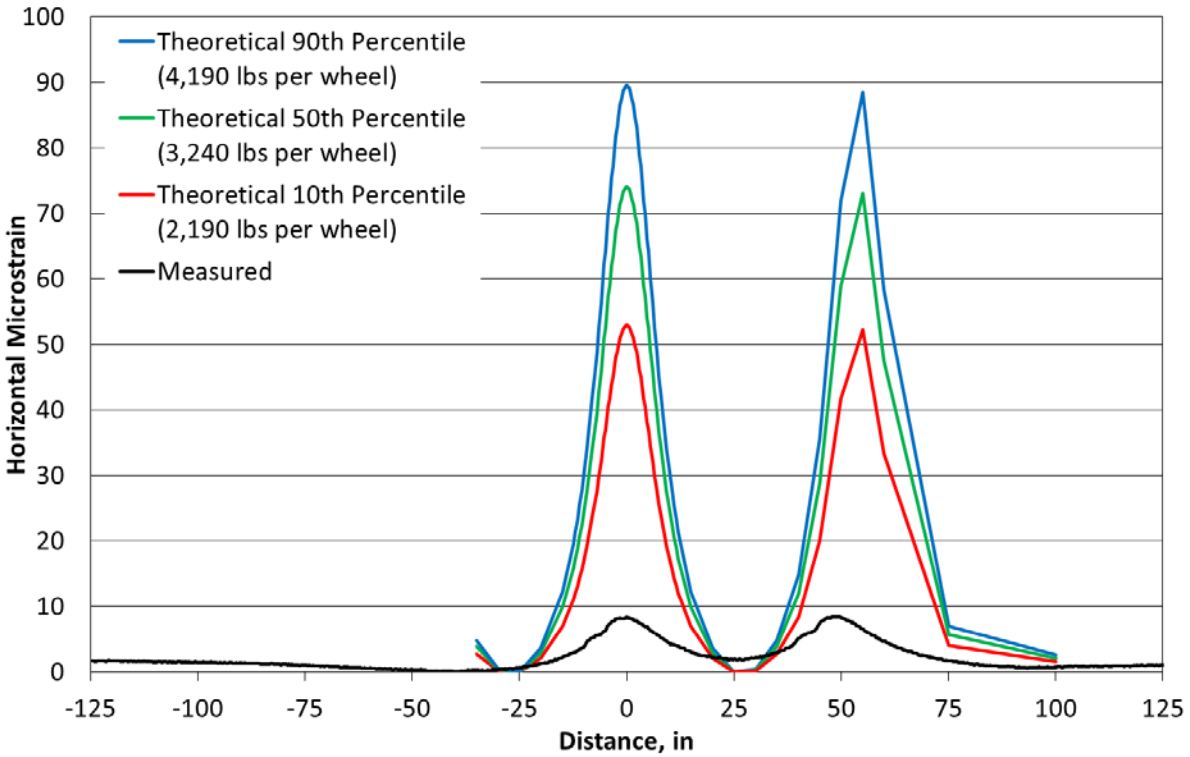

Figure 5.15: Medford Tandem Axle Strain Comparison #1.

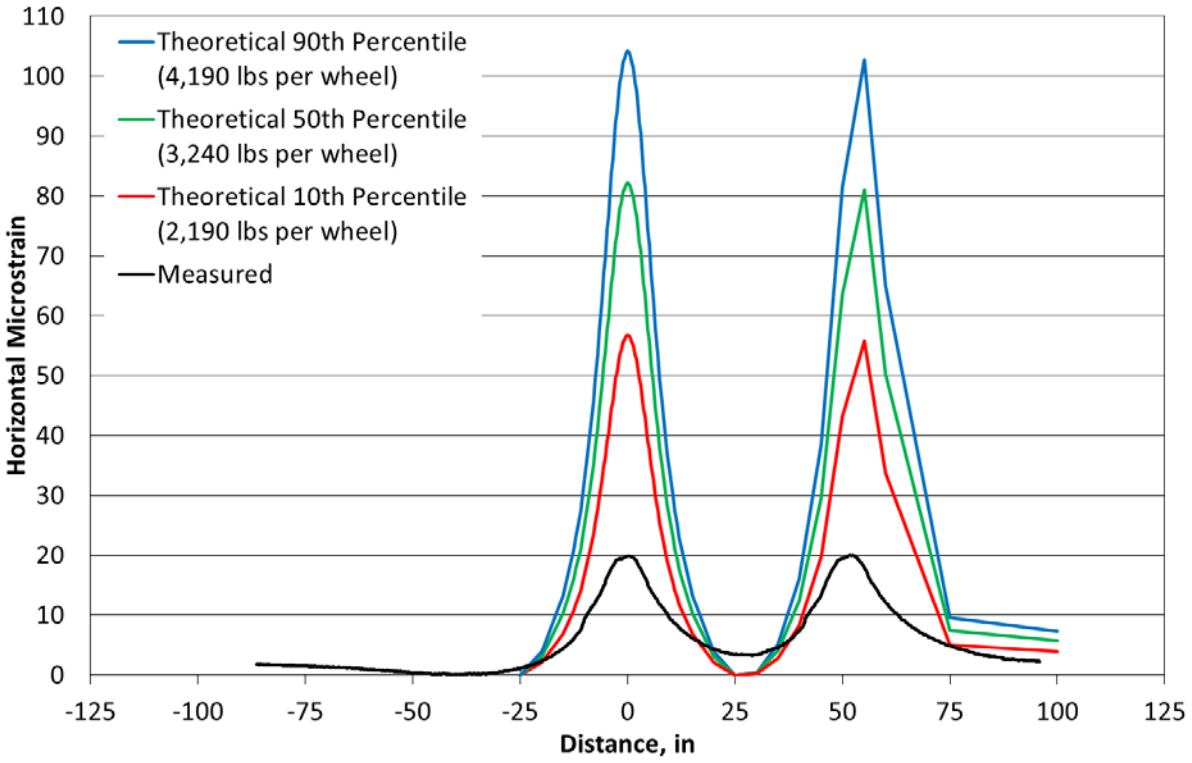

Figure 5.16: Medford Tandem Axle Strain Comparison #2.

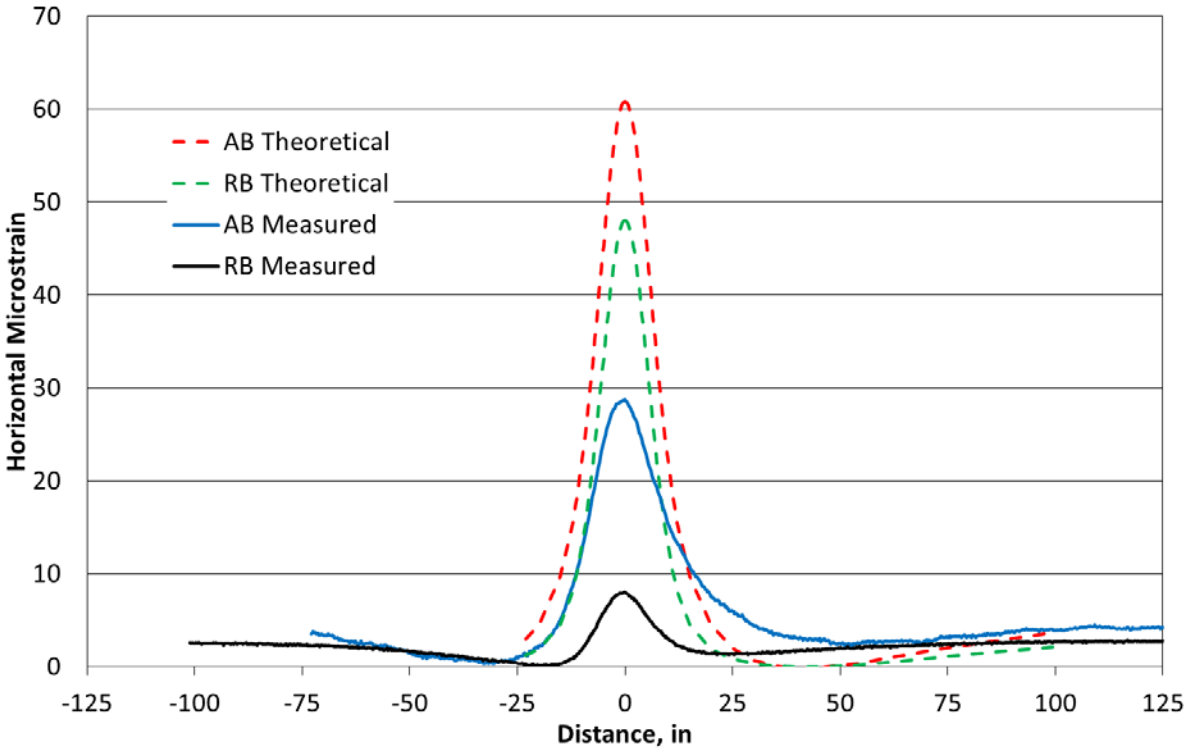

Figure 5.17: Dever-Conner 90th Percentile Steer Axle Strain Comparisons.

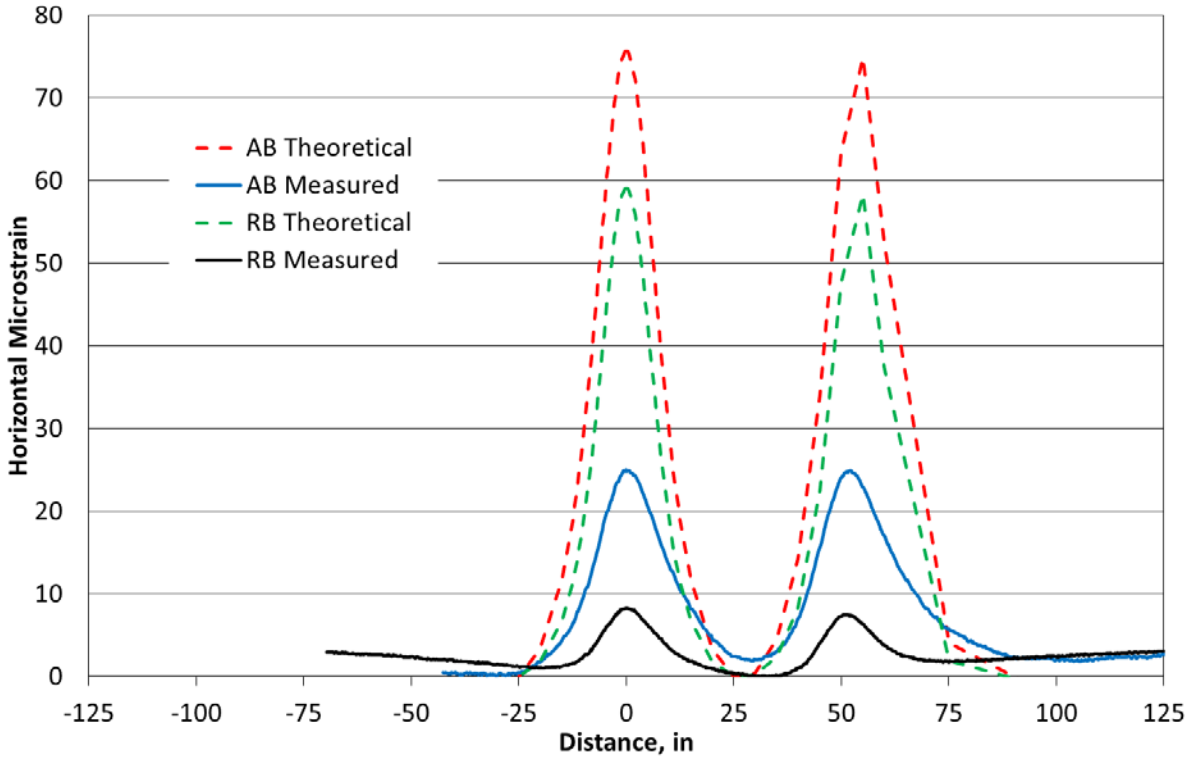

Figure 5.18: Dever-Conner 90th Percentile Tandem Axle Strain Comparisons.

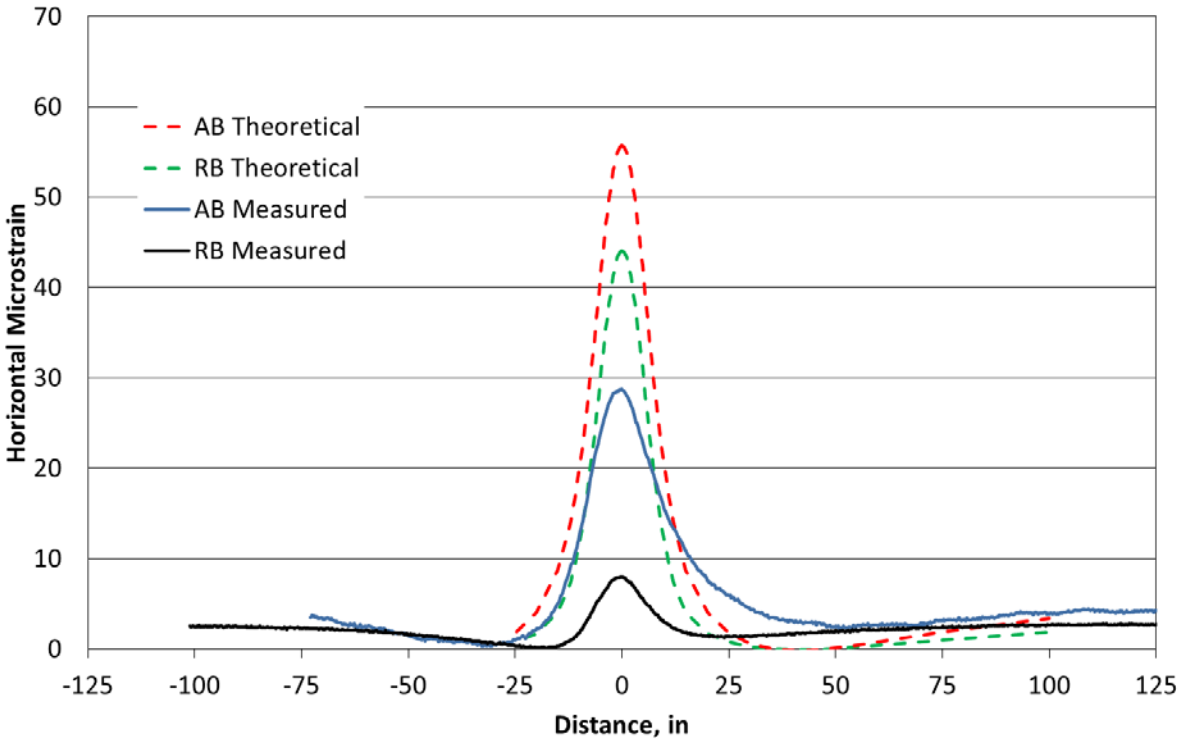

Figure 5.19: Dever-Conner 50th Percentile Steer Axle Strain Comparisons.

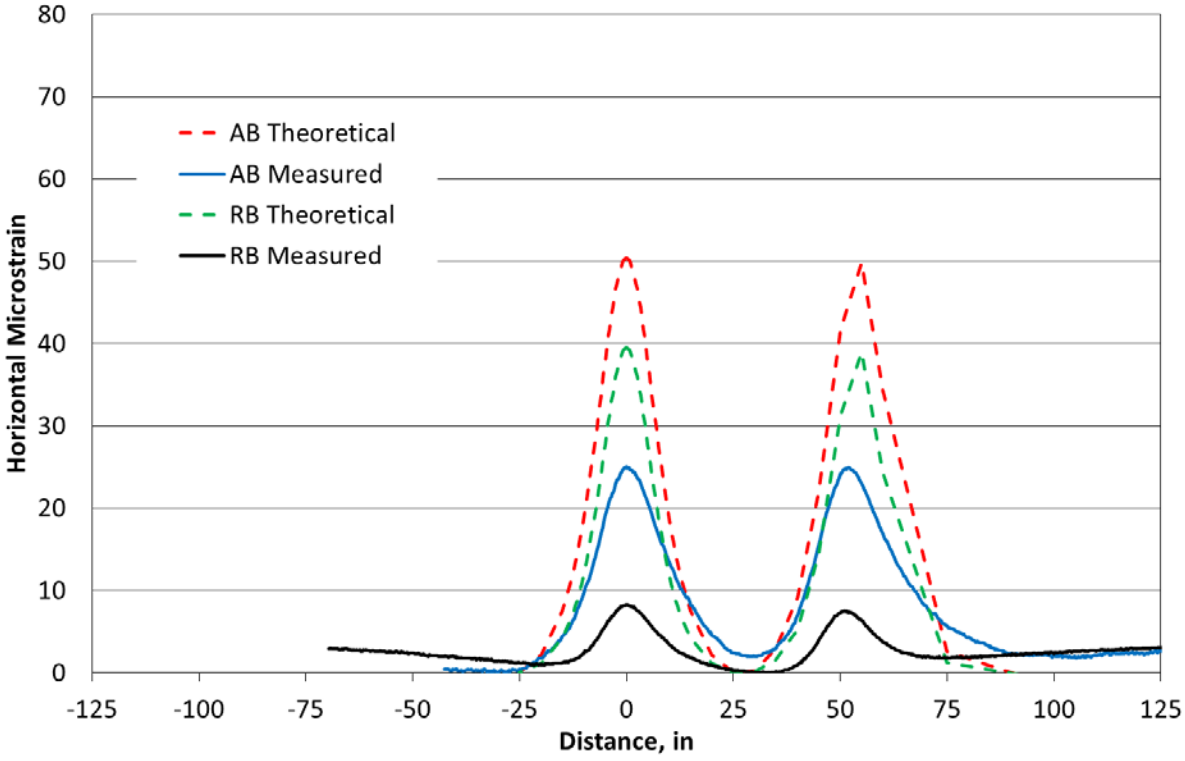

Figure 5.20: Dever-Conner 50th Percentile Tandem Axle Strain Comparisons.

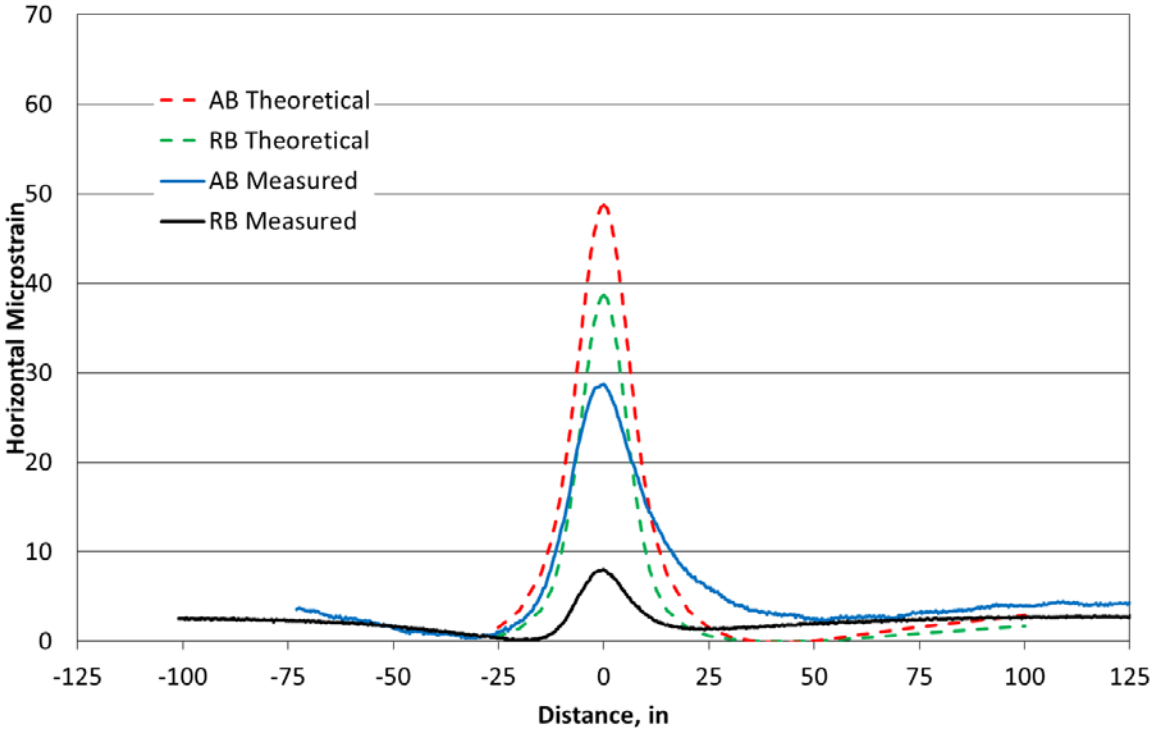

Figure 5.21: Dever-Conner 10th Percentile Steer Axle Strain Comparisons.

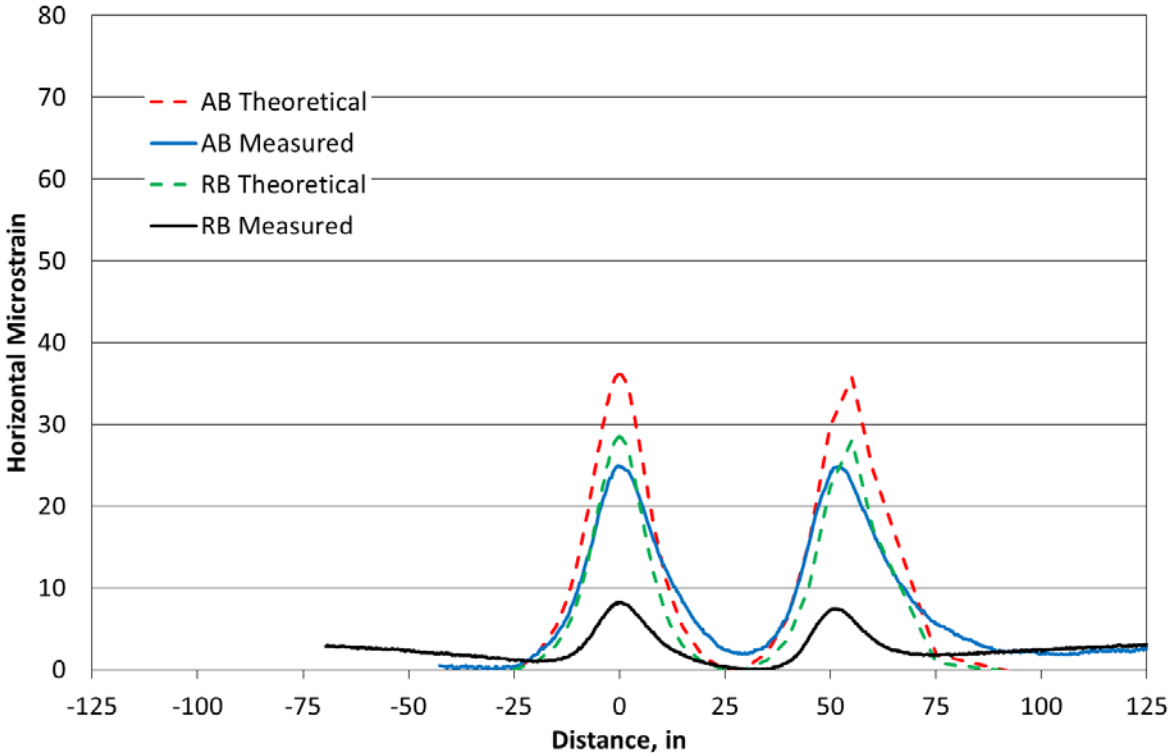

Figure 5.22: Dever-Conner 10th Percentile Tandem Axle Strain Comparisons.

5.6 FURTHER INVESTIGATIONS

As noted previously, the material property inputs for simulation were fixed based on WESLEA default values. These properties, also noted previously, have an impact on the computed strain levels. To demonstrate the effect on the JRCP rubblized base material, the modulus was varied to find a better match of the strain reduction observed in the measured responses. A range of modulus values from 100,000 psi to 1,000,000 psi was obtained from the 2006 ODOT Pavement Design Guide *(ODOT 2006)*. It can be seen in Figures 5.23 and 5.24 that as the modulus is increased the strain decreases. Assuming all of the other inputs are correct, the in-situ modulus of the rubblized JRCP base is likely between 500,000 psi and 1,000,000 psi under these conditions.

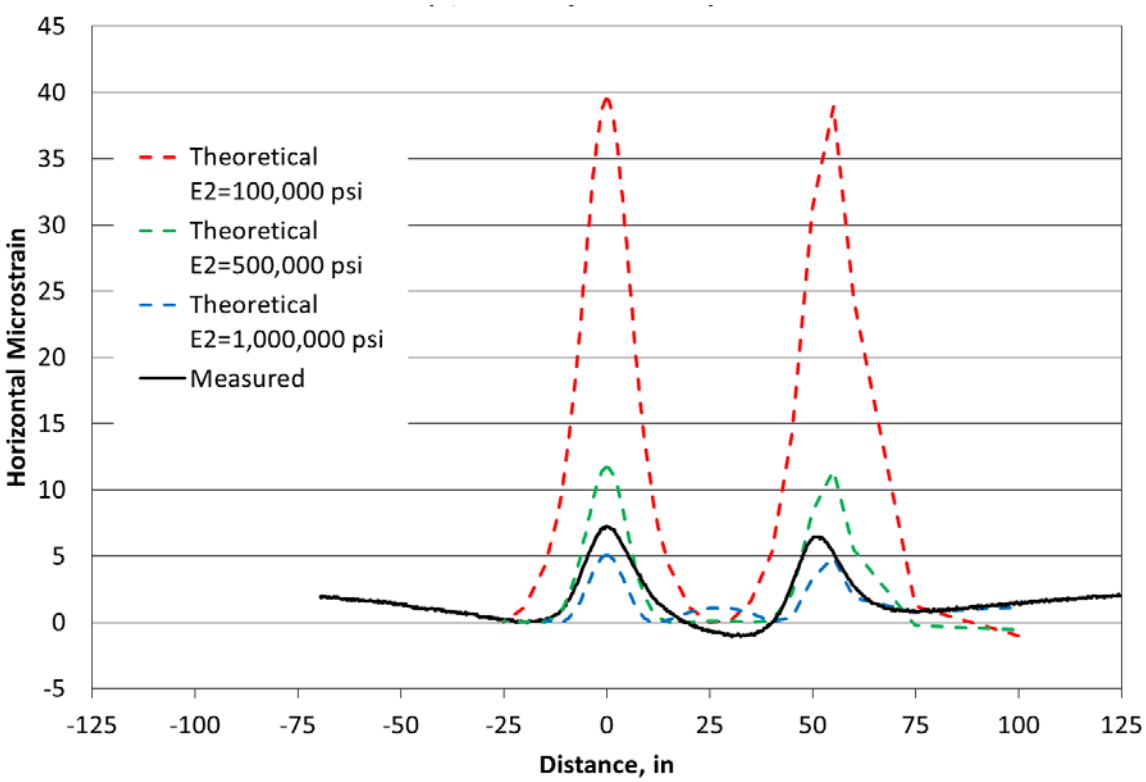

Figure 5.23: Dever-Conner Rubblized JRCP Modulus Strain Comparison #1.

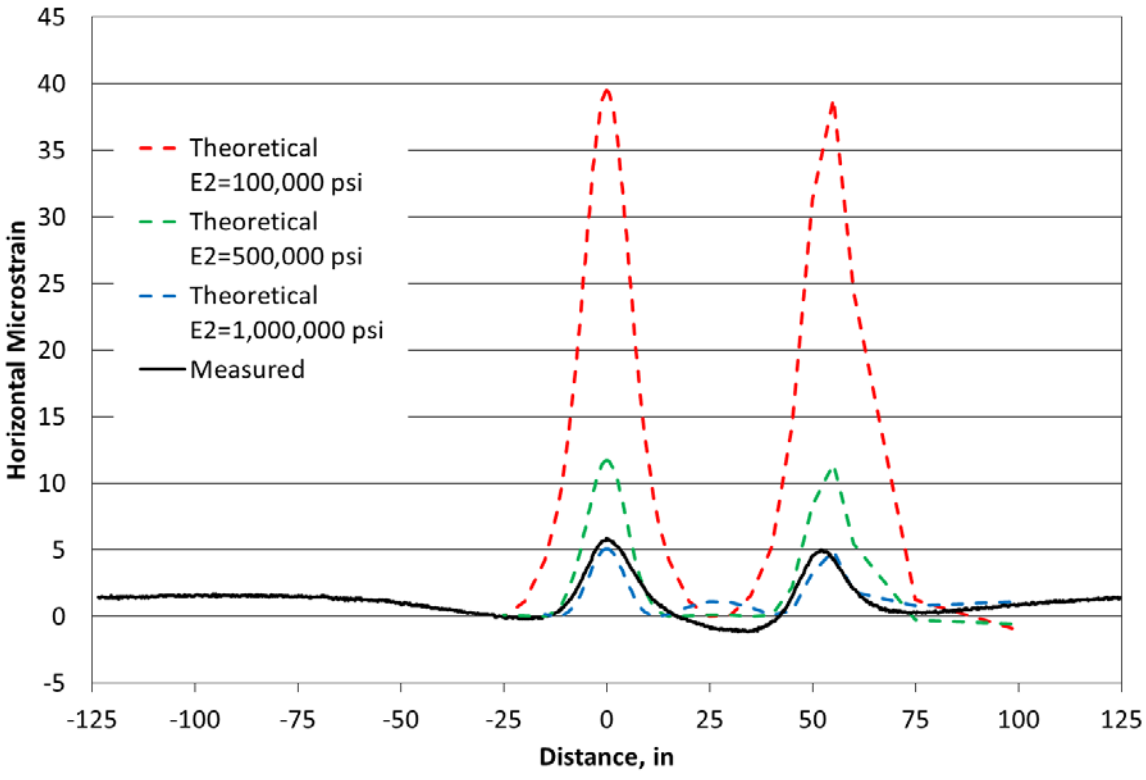

Figure 5.24: Dever-Conner Rubblized JRCP Modulus Strain Comparison #2.

To further examine the benefit of the rubblized base at the Dever-Conner site, the strain levels generated by a single vehicle event over each base type were compared. It can be seen in Figure 5.25 that the strain magnitudes were significantly reduced by the rubblized JRCP. A strain comparison, on a vehicle-by-vehicle basis, for ten 5 axle vehicles is presented in Figure 5.26. A large reduction in strain from the aggregate base to the rubblized base was seen in all vehicles and axle types. The corresponding percent reduction for each axle type of each vehicle is shown in Figure 5.28. An average of 70% strain reduction was found across all 10 trucks and both axle types.

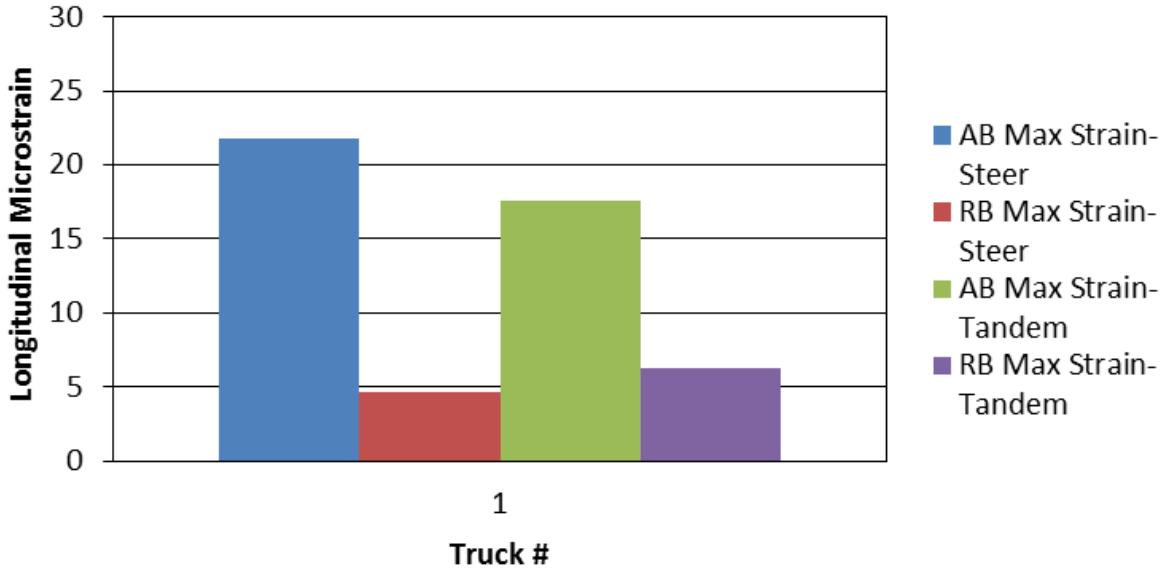

Figure 5.25: Dever-Conner Single Vehicle Base Layer Strain Comparison

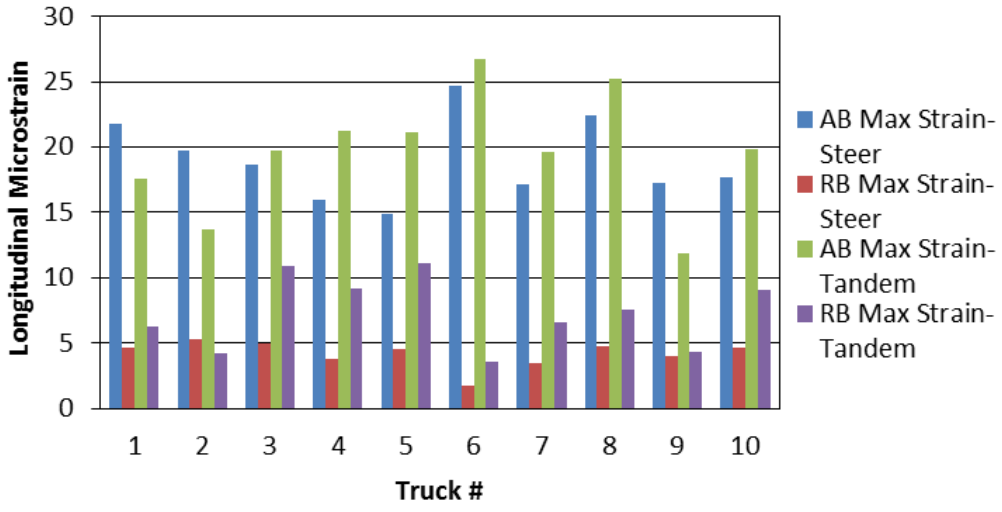

Figure 5.26: Dever-Conner Base Layer Strain Comparison

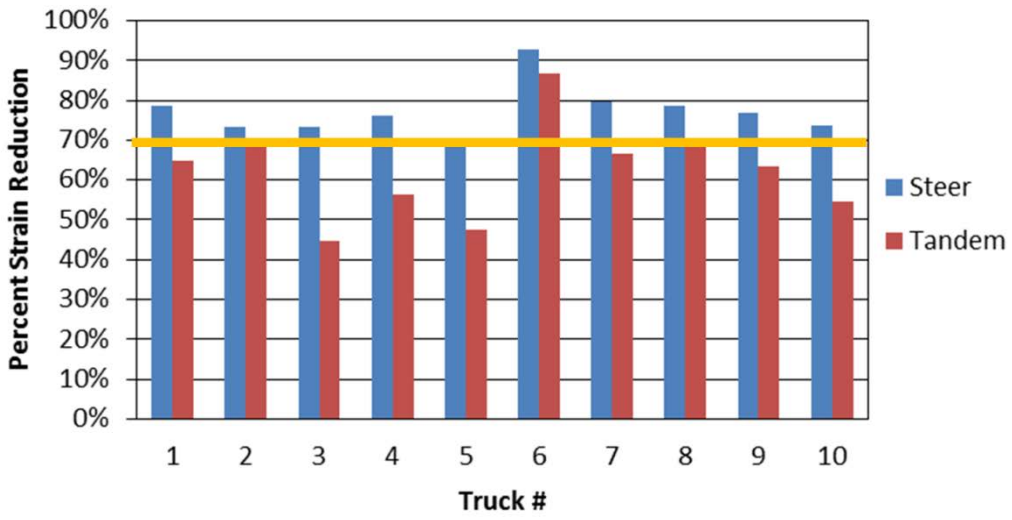

Figure 5.27: Dever-Conner Base Layer Strain Reduction

6.0 CONCLUSIONS AND RECOMMENDATIONS

Based on the information above, the following conclusions and recommendations are made:

1. The collected strain data appear valid. The shapes of the strain signals are as-expected for both longitudinal and transverse strain measurements.

2. Processing schemes developed in DADiSP effectively handle the variety of file formats within this project.

3. There is difficulty in linking WIM-recorded load events to strain events. Though some records do exist for the Dever-Conner site linking the two data sets, other approaches such as matching percentile loads and pavement responses will need to be used to characterize the effects of axle load on pavement response.

4. Results from layered elastic modeling of the pavement sections matched the measured results qualitatively. Imprecise loading and material property information prevented a quantitative assessment of the data.

5. The Dever-Conner site provided valuable information on the effectiveness of rubblized base in controlling strain levels relative to an aggregate base course.

6. There appears to be sufficiently valid data, from each of the three sites, to warrant Phase II of this project that will include fully processing the remaining data files and building a database to store the data and facilitate analysis.

7.0 REFERENCES

Scholz, T.V. *Instrumentation for Mechanistic Design Implementation*. Final Report, OTREC-RR-10-02, Oregon Transportation Research and Education Consortium (OTREC), 2010.

Timm, D.H., and A.L. Priest. *Wheel Wander at the NCAT Test Track*. Report No. 05-02, National Center for Asphalt Technology, Auburn University, 2004.

Oregon Department of Transportation. *ODOT Pavement Design Guide*. Pavement Services Unit, Oregon Department of Transportation, 2006.